U.PORTO

2º CICLO EM MEDICINA E ONCOLOGIA MOLECULAR
CIÊNCIAS DA SAÚDE

Human Zona Pellucida and Cancer

Jéssica Sofia Mateus Costa

M

2018

U.PORTO

FMUP FACULDADE DE MEDICINA
UNIVERSIDADE DO PORTO

HUMAN ZONA PELLUCIDA AND CANCER

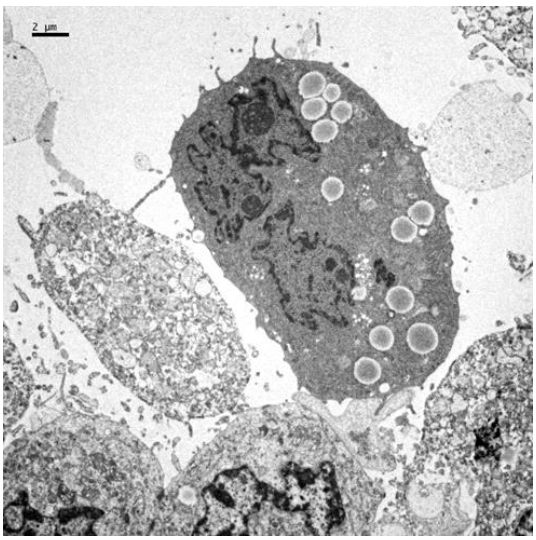

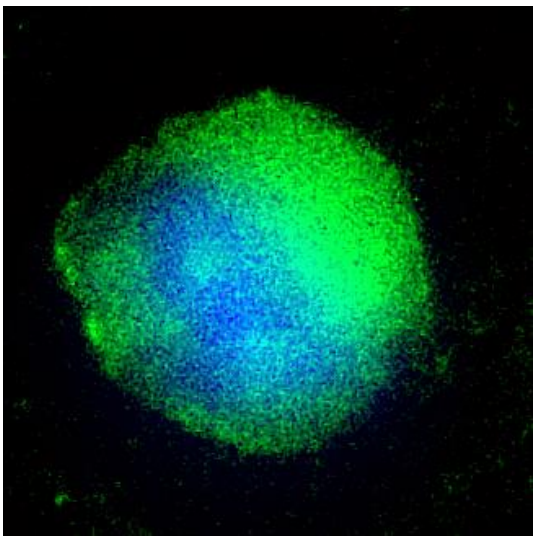

Jéssica Sofia Mateus Costa

DISSERTAÇÃO DE MESTRADO APRESENTADA

À FACULDADE DE MEDICINA DA UNIVERSIDADE DO PORTO EM

MEDICINA E ONCOLOGIA MOLECULAR

Faculdade de Medicina da Universidade do Porto

Human Zona Pellucida and Cancer

Dissertação de Mestrado em Medicina e Oncologia Molecular

Jéssica Sofia Mateus Costa

Orientador: **Professora Doutora Rosália Sá, PhD, Professora Auxiliar**

Laboratório de Biologia Celular, Departamento de Microscopia

Unidade Multidisciplinar de Investigação Biomédica (UMIB)

Instituto de Ciências Biomédicas de Abel Salazar (ICBAS), Universidade do Porto

ORCID ID**:** 0000-0002-6551-3822

Coorientador: **Professor Doutor Mário Sousa, MD, PhD, Professor Catedrático**

Laboratório de Biologia Celular, Departamento de Microscopia

UMIB, ICBAS-UP

ORCID ID: 0000-0002-3009-3290

Porto 2018

Dissertação de candidatura ao grau de Mestre em Medicina e Oncologia Molecular submetida à Faculdade de Medicina da Universidade do Porto.
O presente trabalho foi desenvolvido no Instituto de Ciências Biomédicas Abel Salazar, sob a orientação científica da Professora Doutora Rosália Maria Pereira de Oliveira e Sá e coorientação do Professor Doutor Mário Manuel da Silva Leite Sousa

Dissertation of candidacy for the degree of Master in Medicine and Molecular Oncology submitted to the Faculty of Medicine of the University of Porto.
The present work was developed at the Institute of Biomedical Sciences Abel Salazar under the scientific supervision of Rosália Maria Pereira de Oliveira e Sá, PhD and co-orientation of Mário Manuel da Silva Leite Sousa, MD, PhD

Aqueles que passam por nós, não vão sós, não nos deixam sós.
Deixam um pouco de si, levam um pouco de nós.

Antoine de Saint-Exupéry

Publicações e comunicações durante a frequência do Mestrado

Publicações Internacionais

Artigo Prático:

Costa J, Pereira R, Oliveira J, Alves A, Magalhães A, Frutuoso A, Leal C, Barros N, Fernandes R, Barreiro M, Barros A, Sousa M, Sá R (**2018**). Structural and molecular analysis of the cancer prostate cell line PC3: oocyte zona pellucida glycoproteins. **Tissue Cell** (submitted).

Comunicações Nacionais

Costa JM, Malhão F, Sousa M and Sá R (2016) Ultrastructural Analysis of Human Prostatic Cancer Cells in Suspension. 50th Meeting of the Portuguese Microscopy Society: ‘’Microscopy and Microanalysis in Materials and Life Sciences’’, Institute of Biomedical Sciences Abel Salazar, University of Porto, Porto, Portugal, June 29 – 30 (oral presentation).

Experiência pedagógica e de supervisão

Monitora do estágio ‘’Zona Pelúcida - Um contracetivo?”, no âmbito do 13.º Congresso da Escola de Ciências da Vida e da Saúde (ECVS) – Universidade Júnior, que decorreu no Instituto de Ciências Biomédicas de Abel Salazar (ICBAS) da Universidade do Porto, entre os dias 4 e 9 de setembro de 2017.

Monitora da atividade ‘O médico que apenas sabe medicina, nem medicina sabe”, no âmbito dos cursos de verão da Universidade Júnior, que decorreu no Instituto de Ciências Biomédicas de Abel Salazar (ICBAS) da Universidade do Porto, entre os dias 17 e 28 de julho de 2017.

Monitora da atividade ‘’Do sintoma à investigação”, no âmbito dos cursos de verão da Universidade Júnior, que decorreu no Instituto de Ciências Biomédicas de Abel Salazar (ICBAS) da Universidade do Porto, entre os dias 3 e 14 de julho de 2017.

Monitora do estágio curricular integrado na disciplina de ‘’Formação em Contexto de Trabalho, do Colégio Internato dos Carvalhos, no ano letivo de 2016/2017, com a duração de 280 horas.

Monitora do estágio ‘’Zona Pelúcida - Um contracetivo?”, no âmbito do 12.º Congresso da Escola de Ciências da Vida e da Saúde (ECVS) – Universidade Júnior, que decorreu no Instituto de Ciências Biomédicas de Abel Salazar (ICBAS) da Universidade do Porto, entre os dias 5 e 10 de setembro de 2016.

Cursos/Formações

Participação no 2º Encontro Técnico de Microscopia Eletrónica – ‘’Histochemistry in Electron Microscopy: Techniques and Applications”. que decorreu no Instituto de Ciências Biomédicas de Abel Salazar (ICBAS) da Universidade do Porto, no dia 27 de junho de 2017.

AGRADECIMENTOS

Estas páginas resumem dois anos de muita aprendizagem, esforço e dedicação junto das melhores pessoas. Estas foram imprescindíveis nesta etapa e que como tal merecem o meu maior agradecimento.

À Professora Doutora Rosália Sá, obrigada por me receber e apostar em mim. Agradeço todos os ensinamentos e oportunidades que me permitiram crescer. Sem dúvida alguma, aprendi e cresci imenso. É incansável e um exemplo de determinação que nunca esquecerei.

Ao Professor Doutor Mário Sousa, por acreditar em mim e me dar esta oportunidade. Obrigada por me ensinar que simplificar muitas vezes é melhor forma de ver com clareza os resultados e fazer um bom trabalho.

À Faculdade de Medicina da Universidade do Porto (FMUP), pelo ano probatório rico em conhecimento nas mais variadas áreas. Obrigada aos Professores, nomeadamente ao Professor Henrique Almeida, pela oportunidade de embarcar neste Mestrado de renome e por toda a sabedoria que me transmitiram. À Faculdade, um agradecimento especial pelo financiamento disponibilizado, muito útil na realização desta tese.

Ao Instituto de Ciências Biomédicas Abel Salazar (ICBAS), por me dar as melhores condições de trabalho e as pessoas mais competentes e incríveis para me acompanhar na realização da minha dissertação.

Ao Instituto Português de Oncologia do Porto, nomeadamente ao Professor Rui Henrique, à Professora Doutora Cármen Jerónimo e à Ângela Magalhães, pelo material disponibilizado e pela pronta ajuda.

Ao Centro Materno Infantil do Norte/Centro Hospitalar do Norte, em particular à Doutora Márcia Barreiro (Médica especialista em Ginecologia e Obstetrícia, Diretora da Unidade de Medicina da Reprodução) e à Doutora Carla Leal (Embriologista Sénior) e ao Centro de Genética da Reprodução Prof. Alberto Barros, nomeadamente à Doutora Joaquina Silva (Médica, Embriologista Sénior) pelas amostras cedidas e pela disponibilidade.

Ao Hospital Pedro Hispano, nomeadamente ao Professor Doutor Amaro Frutuoso, por todas as amostras e reagentes facultados, pela ajuda constante e disponibilidade.

À Elsa, obrigada por partilhar comigo a sua mestria na área da microscopia eletrónica e na manipulação de ovócitos. Obrigada por me ensinar a ver sempre os dois lados da moeda e por todos os sábios conselhos. É um exemplo de que a experiência nos faz crescer não só a nível laboratorial como também a nível pessoal.

À Ângela, a minha super-heroína do laboratório, sempre pronta a ajudar. Obrigada por me ensinares a relativizar e me mostrares que mais importante que onde queremos chegar, é o caminho até lá. És uma pessoa genuinamente boa e dona de um coração gigante cujo exemplo levarei para a vida toda.

À Rute, a minha luz ao fim do túnel. Chegaste já no fim do meu percurso, mas marcaste bem o teu lugar. Foste uma ajuda preciosa e não tenho palavras para agradecer todos os teus ensinamentos e o que fizeste por mim. Sei que já o disse mil vezes, mas, novamente, obrigada!

À Sónia, dona de uma perseverança e persistência indestrutíveis. Obrigada por seres uma fonte de inspiração e me provares que com muito trabalho o sucesso é garantido.

À Fernanda e à Célia, a dupla imbatível. Admiro a vossa sede pelo conhecimento e agradeço toda a vossa ajuda a responder às minhas infindáveis dúvidas. Obrigada pelos preciosos conselhos.

Às minhas eternas 'professoras' Madalena e Carla, por terem sempre um sorriso aberto e por estarem sempre disponíveis para esclarecer as minhas questões.

Aos vizinhos da Biologia Molecular e Citogenética, pela companhia na tempestade e na bonança.

À Inês, ao Saulo e todos os alunos que tive o prazer de ensinar na Universidade Júnior e ECVS, são sem dúvida o que me faz mover. Obrigada por me deixarem ser a vossa monitora Jéssica e por me ensinarem que a transmissão de conhecimento é sempre bidirecional.

À Vera, Diogo, Inês e ao Pedro, aos quais tive o privilégio de ajudar na realização das suas teses e que deixaram de uma forma ou de outra uma marca no meu caminho.

À Jedi, a minha companhia de todos os dias. O meu miminho ao acordar e ao fim do dia. Foi bom poder desabafar contigo por mais que saiba que não me entendes. Apesar de me tirares do sério, foste essencial para manter a minha sanidade mental.

À minha Mãe, pelo exemplo de força que és. Apesar da distância estiveste sempre presente e sempre pronta a ouvir os meus desabafos. Mesmo travando as tuas batalhas e mesmo não entendendo nada do meu mundo, estiveste sempre presente. Não há conselhos mais sábios que os teus. Obrigada por acreditares em mim e me deixares voar. És tudo para mim.

Ao Diogo, obrigada por cresceres comigo, por tentares me compreender mesmo quando nada faz sentido. Obrigada por me chamares à razão. Apesar de longe, tentaste sempre dar o teu melhor para me ajudar e apesar de não o mostrar, eu reconheço. Obrigada pelo teu amor e companhia, juntos somos mais fortes.

Às minhas irmãs, Daniela, Cindy e Magali, vocês são tão pequenas e tão importantes para mim. São o que me faz querer ser melhor todos os dias, querer ser um exemplo para vocês. Obrigada pela vossa ingenuidade, pelo vosso sorriso e pelo ''mana Jé" que me derrete o coração.

Às minhas companheiras de fim de dia, obrigada por me ouvirem pregar todos os meus desabafos e aventuras. À Liliana, coração que transborda e exemplo de um líder que arregaça as mangas e vai ao trabalho. Obrigada pelo exemplo de pessoa que és. À Juliana, por me aturares mesmo quando não me calo, por partilhares e compreenderes os meus dilemas. À Patrícia, por me receberes sempre com um ''cheguei!'' e por estares sempre pronta a me ensinar mais. És uma ótima ouvinte e conselheira. À Marisa, obrigada por partilhares a base da cadeia alimentar comigo e me ensinares o que toda a gente se esquecia. Foi um privilégio te conhecer e te ver crescer, obrigada por esse sorriso ''super melhor amiga''.

Aos meus colegas da Cruz Vermelha Portuguesa do Porto, pelas experiências, aprendizagem e imensas histórias para contar. À Cruz Vermelha Portuguesa agradeço a possibilidade de fazer crescer o meu lado mais humanitário e a oportunidade de ajudar o próximo.

À Cátia, Raquel e Sara que por mais longe que tivessem e por mais difícil que fosse marcar um encontro, estiveram sempre presentes e prontas a ajudar.

RESUMO

A zona pelúcida (ZP) humana é uma estrutura acelular glicoproteica que reveste o ovócito e o embrião até ao momento da implantação uterina. Constituída por quatro glicoproteínas – ZP1, ZP2, ZP3 e ZP4 – é uma matriz com um papel muito importante no desenvolvimento folicular, na fertilização e no desenvolvimento embrionário inicial. Focando nas proteínas que constituem a ZP é importante salientar que todas possuem na sua constituição um domínio denominado ZP. Este domínio está também presente noutras proteínas além das glicoproteínas da ZP. As proteínas contendo o domínio ZP são designadas de proteínas com o domínio ZP (do inglês ZP-domain proteins).

Recentemente, estudos têm vindo a associar as proteínas com domínio ZP ao cancro. Alguns investigadores demonstraram a expressão da proteína ZP3 no cancro da próstata e do ovário. Esta descoberta permitiu o desenvolvimento de uma terapia baseada na imunização contra a proteína ZP3 com regressão da massa tumoral e diminuição da sua capacidade invasora e metastática.

Com base nestes resultados promissores, decidimos investigar se o carcinoma da próstata e uma das linhas celulares derivada do carcinoma da próstata (PC3) expressam do mesmo modo as restantes proteínas que compõem a estrutura da ZP. Em primeiro lugar, realizamos a caracterização da ultraestrutura das células da linha celular humana PC3 onde se observou dois tipos de crescimento, um crescimento aderente (células pavimentosas) e um crescimento em suspensão (células em agregados). Observou-se ainda que as células pavimentosas e as células em agregados diferem ultraestruturalmente e apresentam algumas características ultraestruturais semelhantes ao tecido tumoral e outras características que ainda não foram descritas.

A expressão das proteínas ZP1-ZP4 foi avaliada por imunohistoquímica no tecido de carcinoma da próstata e por imunocitoquímica nos dois tipos de células da linha celular PC3. Observou-se a expressão de todas as proteínas da ZP tanto no tecido tumoral como nas células e não se observou positividade no tecido prostático normal.

A expressão dos genes ZP1-ZP4 foi também avaliada em ambas as células pavimentosas e agregadas por métodos de biologia molecular. Nestes ensaios foi possível confirmar a expressão dos genes ZP1, ZP3 e ZP4 em ambas as células. A avaliação quantitativa por PCR permitiu concluir que o gene ZP3 é o mais expresso, seguido da ZP1 e ZP4. Observou-se ainda que as células pavimentosas apresentam uma expressão maior dos genes ZP1, ZP3 e ZP4 face às células em agregados.

Neste trabalho apresentamos uma descrição detalhada da ultraestrutura das células da linha celular PC3 e mostramos a expressão das proteínas ZP1-ZP4 no tecido e células tumorais da próstata. No entanto, mais estudos precisam de ser realizados de forma a entender qual o

mecanismo que leva à expressão das proteínas da ZP no tecido e células tumorais e esclarecer as suas possíveis funções na célula.

Palavras-chave: Zona pelúcida; Cancro da próstata; linha celular neoplásica prostática PC3; Ultraestrutura; Imunocitoquímica; PCR quantitativo.

ABSTRACT

The human zona pellucida (ZP) is an acellular structure that surrounds the oocyte and the developing embryo untill the moment of uterine implantation. The ZP is an extracellular matrix constituted by four glycoproteins (ZP1, ZP2, ZP3 and ZP4) with important roles in folliculogenesis, fertilization and in the embryo early development. Focusing on the proteins that constitute the ZP it is important to emphasize that all of them have in their composition a domain called ZP-domain. The ZP-domain is also present in other proteins besides ZP glycoproteins. The proteins that have the ZP-domain are named ZP-domain proteins.

Recent studies have been associating ZP-domain proteins with cancer. Some researchers have shown the expression of the ZP3 protein in prostate and ovarian cancer. These findings allowed the development of a new therapy based on the immunization against the ZP3 protein that lead to regression of the tumoral mass and decreased invasion and metastasis.

Based on these promising results, we decided to investigate if prostatic carcinoma and one of the cell-lines derived from prostatic carcinoma (PC3) express, in the same way, the remaining proteins that make up the ZP structure. First, we characterized the ultrastructure of the cells from the PC3 cell-line where it was possible to observe two types of growth, one adherent (pavement-cells) and one in suspension (aggregated-cells). We also observed that pavement and aggregated cells differed from one another ultrastructurally and have some characteristics that are similar to the prostatic carcinoma tissue and other characteristics that have not been described.

The expression of the ZP1-ZP4 proteins was evaluated by immunohistochemistry in the tissue from prostate carcinoma and by immunocytochemistry in both pavement and aggregated cells of the PC3 cell-line. The expression of the ZP1-ZP4 proteins was detected in both tumoral tissue and cells. It was not observed any positivity in the normal prostatic tissue.

ZP1-ZP4 gene expression was also evaluated on both adherent and aggregated cells by molecular biology methods. These assays confirm the expression of the ZP1, ZP3 and ZP4 genes in both cell types. The quantitative evaluation by RT-PCR revealed that the ZP3 gene is the most expressed, followed by ZP1 and ZP4 genes. Also, pavement cells present higher expression levels of the ZP1, ZP3 and ZP4 genes when compared with aggregated cells.

In this work we present a detailed description of the ultrastructure of the cells from the PC3 cell-line and reveal the expression of the ZP1-ZP4 proteins in the prostate cancer tissue and tumor cells. Nevertheless, further studies are required in order to understand the mechanism behind the expression of the ZP1-ZP4 proteins in the tumoral tissue and cells, and elucidate the plausible mechanisms of these proteins in the cell.

Keywords: Zona pellucida; Prostate cancer; prostate cancer cell-line PC3; Ultrastructure; Immunocitochemistry; RT-PCR

TABLE OF CONTENTS

LIST OF TABLES

LIST OF FIGURES

LIST OF ABBREVIATIONS

ART	Assisted Reproductive Technology
CD105	Cluster of differentiation molecule 105
CFCS	Consensus furin cleavage site
CHP	Hospital Center of Porto
CMIN	Maternal Child Center of the North
CUB	Complement C1r/C1s, Uegf, Bmp1
CUZD1	CUB and zona pellucida-like domains-containing protein 1
D8C	Domain of eight cysteines
DAB	Diaminobenzidine
DAPI	4′,6-diamidino-2-phenylindole
DMBT1	Deleted in malignant brain tumors-1
DNA	Deoxyribonucleic acid
EGF	Epidermal growth factor
ELISA	Enzyme-linked immunosorbent assay
FBS	Fetal bovine serum
FITC	Fluorescein isothiocyanate
HPA	Human protein atlas
IC	Immunocitochemistry
IH	Immunohistochemistry
IVF	In-vitro fertilization
LOH	Loss of heterozygosity
NCBI	National center for biotechnology information
PAS	Periodic acid Schiff
PBS	Phosphate buffer saline
PCR	Polymerase chain reaction
PLAC	Placenta-specific 1
RER	Rough endoplasmic reticulum
RNA	Ribonucleic acid

RPMI	Roswell park memorial institute medium
RXRR	Protein sequence Arginine-Any amino acid-Arginine-Arginine
SRCR	Scavenger receptor cysteine-rich
SRRR	Protein sequence Serine- Arginine-Arginine-Arginine
SS	Signal sequence
TCR	T-cell receptor
TEM	Transmission electron microscopy
TGF-β1	Transforming growth factor beta 1
TMB	Transmembrane domain
ZP	Zona pellucida

I. INTRODUCTION

1. The human zona pellucida

The Zona pellucida (ZP) is an acellular matrix that surrounds the oocyte and the developing embryo until uterine implantation of the blastocyst. The ZP is composed by four glycoproteins (ZP1-ZP4) that polymerize and guarantee the important functions of ZP, which include, among others, the promotion of follicle development in the ovary, the sperm-oocyte interaction, and the protection of the developing embryo from mechanical stress and immune rejection. A common characteristic between the four ZP glycoproteins is the presence of a protein domain named ZP-domain. Besides the ZP1-ZP4 proteins, other proteins have been described to share the same ZP-domain. Increasingly number of studies have demonstrated an association between ZP-domain proteins and cancer.

1.1. Structure

The human ZP is an extracellular glycoprotein matrix composed of four glycoproteins ZP1, ZP2, ZP3 and ZP4 (Lefièvre *et al.*, 2004). These proteins are encoded by four distinct genes ZP1-ZP4 located on chromosomes 11, 16, 7 and 1, respectively (Hughes & Barratt, 1999).

Zona pellucida glycoproteins are highly conserved among species and share several domains (Gupta *et al.*, 2012), such as a ZP domain, a transmembrane like-domain, a N-terminal signal sequence, and a C-terminal propeptide that is removed by a protease sensitive region. Human ZP glycoproteins also share a consensus furin cleavage site (CFCS) where protein precursors are cleaved by furin and switch to the active state. This consensus cleavage site on ZP1-ZP3 proteins is the amino acid sequence Arginine-Any amino acid-Arginine-Arginine (RXRR), while in the human ZP4 the protein sequence is Serine-Arginine-Arginine-Arginine (SRRR). Human ZP1 and ZP4 share a trefoil domain likewise, which is absent from ZP2 and ZP3. Goudet and colleagues (2008), suggested that ZP4 is a paralog of ZP1 and that they may play similar roles since seem to have evolved from a common ancestor through duplication (Goudet *et al.*, 2008).

Zona pellucida proteins are synthesized in the endoplasmic reticulum of oocyte and granulosa cells and are actively secreted to support folliculogenesis (Gook *et al.*, 2008). Repeating units of ZP2, ZP3 and ZP4 heterodimers are cross-linked by ZP1 dimers to form a paracrystaline three-dimensional network structure (Green, 1997). Under polarized light, the human ZP has an estimated thickness of 19.5 ± 2.2 µm with delimitation of three layers, outer, middle and inner, with approximately 6.1 µm, 3.7 µm and 9.8 µm, respectively (Pelletier *et al.*, 2004). Moreover, studies with transmission electron microscopy showed that the ZP is homogeneously finely fibrillar with numerous remnants of follicular cell feet (Sá *et al.*, 2011; Sousa *et al.*, 2016). Alterations of the human ZP affect a small proportion of retrieved oocytes from Assisted Reproductive Technology (ART) treatment cycles. These alterations are considered

extracytoplasmic oocyte dimorphisms. Extracytoplasmic ZP dimorphisms have a proven impact on ART outcomes as they may compromise the ZP thickness, hardness, density and elasticity (Sousa *et al*., 2015). Still, how the ZP proteins assemble in this filament-based extracellular matrix remains unclear. Jimenez-Movilla and Dean (2011) gave some clues of how ZP proteins incorporate into the ZP. They demonstrated that ZP proteins have cytoplasmic tails that prevent protein oligomerization in the cytoplasm and guide them to the oocyte plasma membrane where they are cleaved at the endoproteinase cleavage site. Then, the remaining protein is released in the extracellular medium where it polymerizes with other ZP proteins and become part of the ZP extracellular matrix (Jimenez-Movilla *et al*., 2011).

1.2. Functions

The ZP history begins in the ovary, more precisely at the primary follicle stage, were ZP proteins begin to be secreted and polymerized in the final ZP structure. Herein, the ZP mediates the connections between the oocyte and follicular cells ensuring an accurate folliculogenesis process (Makabe et al., 2006). After ovulation, the ZP is responsible for the interactions with sperm, where it is essential in the species-specific gamete recognition, in the induction of the acrosome reaction and in polyspermy prevention (Lefièvre et al., 2004; Gupta et al., 2012; Sá et al., 2015).

In the sperm-oocyte interaction, the role of each ZP protein have been studied. It was suggested that ZP1 glycoprotein is responsible for the crosslink between the other ZP proteins, ZP3 is responsible for the primary sperm adhesion/binding and ZP4 assists ZP3 in the induction of the acrosome reaction. ZP2, besides its function as a secondary binding site, is also responsible for the conversion of proacrosin into acrosin, which then helps ZP penetration (Lefièvre et al., 2004; Gupta et al., 2012).

Following fertilization, ZP of the developing embryo endorses the compactation process by promoting the contacts between the embryonic cells. Furthermore, during pre-implantation embryo development, ZP avoids premature implantation, and protects the embryo from mechanical stress and immune rejection (Ewoldsen et al., 1987; Clark et al., 1996; Grasa et al., 2012).

Ultimately, the blastocyst emerges from the enveloping ZP in a phenomenon known as hatching. This phenomenon is imperative for the invasion of the endometrium by blastocyst trophectoderm cells and therefore is essential for implantation (Seshagiri et al., 2016).

1.3. The ZP domain

The ZP-domain consists of approximately 260 amino acids with 8 to 12 cysteine residues that are linked by intramolecular disulfide bonds. Disulfide bonds are frequently present in extracellular or transmembrane proteins where they are important for protein structure

stabilization and protein function and can be used to contact with other proteins of the extracellular environment (Litcher and Wassarman, 2015).

The ZP-domain is predominantly found in the C-terminus of polypeptides and can be divided in two major sub-domains, ZP-N and ZP-C, which are known to have an immunoglobulin-like appearance at high-resolution X-ray crystallography. A protease sensitive region is found between the two ZP sub-domains and several other domains can be present along with the ZP-domain such as: transmembrane domain (TMB), complement C1r/C1s, Uegf, Bmp1 (CUB) domain, scavenger receptor cysteine-rich (SRCR) domain, epidermal growth factor (EGF) domain, and others (Litcher and Wassarman, 2015).

A signal sequence (SS) is present at the N-terminus of the proteins which will follow the secretory pathway either to be allocated at the cell membrane or to be secreted into the extracellular medium. The consensus Furin cleavage site (CFCS) is a short sequence recognized by a proteolytical enzyme of the furin-like family that cleaves the protein in this particular site. Transmembrane domain as the name itself indicates, is a stable hydrophobic domain that can be included in the cell membrane. The CUB domain is a structural motif present in extracellular and plasma membrane associated proteins where it may be responsible for oligomerization and recognition of substrates or binding partners. The SRCR domain is usually associated with the capacity of binding to specific ligands like bacterial and viral pathogens. The EGF domain role is not fully understood but it is believed that its responsible for the binding to specific cell-surface receptors and their dimerization and activation. The nidogen (entactin) domain is an extracellular domain with unknown functions. The Von Willebrand factor type D domain is found in several extracellular and intracellular proteins and is frequently involved in multiprotein complexes where it can have a variety of functions such as cell adhesion, migration, or pattern formation and is known to participate in platelet clotting (Colombatti et al., 1993). The Domain with 8 conserved Cys residues (D8C) is also a domain present in ZP-domain proteins that presents four pair of disulfide bridges that, when disrupted, can lead to protein disfunction (Yang et al., 2004).

ZP-domain proteins, similarly to ZP1-ZP4 proteins, are frequently secreted to the extracellular medium after posttranslational modifications. Besides the already mentioned functions of ZP1-ZP4 proteins, ZP-domain proteins have been associated with other biological functions such as polymerization, cell adhesion, morphogenesis, and cell and cytoskeleton shape remodeling (Plaza et al., 2010).

1.4. Proteins with ZP-domain and Infertility

Some infertility diseases have been related with the ZP. Morphological anomalies that affect the structure, shape and thickness of the ZP have been associated with a poor outcome on ART treatments. To uncover if ZP dimorphisms are associated with mutations on the ZP1-ZP4 genes, several authors analyzed the sequence of ZP genes in oocytes with ZP anomalies versus

morphological normal oocytes (Mannikko et al., 2005; Pokkyla et al., 2011; Yang et al., 2017). It was found that mutations in the ZP2 and ZP3 genes were associated with a greater predisposition for ZP dimorphisms but there was no direct association between the different types of anomalies and a specific mutation.

Missense and nonsense mutations were found in all the four ZP genes and were related to decreased fertility either by a visible alteration in the ZP structure, such as ZP absence (Huang et al., 2014) or a thin ZP (Liu et al., 2017), or by the association with other diseases, like the empty follicle syndrome (Chen et al., 2017) or the polycystic ovary syndrome (Meczekalski et al., 2015). Briefly, mutations in the ZP genes result in misfolded proteins or in the absence of a protein domain that is crucial for protein function.

Autoantibodies against the human ZP proteins were found in the serum and cervical mucus, and were demonstrated to be a source of infertility (Shivers and Dunbar, 1977; Kamada et al., 1984; Hovav et al., 1994; Ulcova-Gallova, 2010; Huo et al., 2015). First, ZP autoantibodies are able to elicit an immune response against the ovary tissue that result in ovarian dysfunction and infertility (Kelkar et al., 2005; Takamizawa et al., 2007). Second, given the important functions of ZP proteins in sperm-oocyte interactions, an antibody anti-ZP can compete for the binding site of the sperm and prevent fertilization (Sacco & Moghissi, 1979; Curtis et al., 1991; Takamizawa et al., 2007).

1.5. Proteins with ZP-domain and Reproductive cancer

In the field of carcinogenesis, ZP3 protein expression was found in ovarian cancer (Rahman et al., 2012) and prostate cancer (Bennink, 2016). These observations enabled the development of new therapeutic strategies for these types of cancer, which are based on the immunization against tumor cells expressing ZP3. This immune response was associated with a decrease in tumor mass and metastasis.

Mice and human granulosa cell tumors also express ZP3 and the vaccination against ZP3 of mice with ovarian tumor lead to an increased humoral and cellular response against the ZP3 antigen (Rahman et al., 2012). This vaccination resulted in weight tumor decrease accompanied by a lack of metastases, autoimmune oophoritis and other side effects. This study reveals a novel strategy for immunotherapy of malignancies that express ZP proteins. Nevertheless, studies in humans are lacking.

Over expression of the *CUB and Zona Pellucida-like Domain-1* (CUZD1) gene was found in ovarian cancer and in an ovarian cancer cell-line by immunohistochemistry and semiquantitative polymerase chain reaction (sqPCR) (Leong et al., 2004). Authors also exposed ovarian cancer cells to anti-CUZD1 serum and observed a decrease in cell attachment and proliferation, suggesting a potential role of this ZP-domain protein in the interactions between the cell and its environment. Later, the same authors performed a gene silencing assay in an ovarian cancer cell-

line, where CUZD1 was silenced using small interfering ribonucleic acid (siRNA) (Leong et al., 2007). Authors found that CUZD1 silencing decreased cell growth and proliferation and increased cisplatin sensitivity. Cisplatin is a chemotherapy drug used to treat ovarian cancer and is associated with the development of drug resistance. In this study, authors also showed that the exposure of cells to cisplatin decreased CUZD1 levels in a dose-dependent manner. Leung et al (2012) measured, by a commercial enzyme-linked immunosorbent assay (ELISA), CUZD1 levels in the serum of late stage ovarian cancer patients. Authors found that CUZD1 levels were elevated in ovarian cancer serum with a high correlation with the cancer antigen 125 (CA-125), an already used ovarian cancer biomarker.

Elevated serum levels of CUZD1 were also found in breast and lung cancer but, in this case, a smaller sample was used (for review see: Liaskos et al., 2013). Shortly after, Prassas et al (2014) demonstrated an unspecific reactivity of the ELISA commercial kit used by Leung et al (2012). Authors found that the detected protein did not match the predicted molecular weight of CUZD1 protein and, instead, it was detecting the CA-125 protein. These results proved the need of caution about results and further studies will be needed to confirm if CUZD1 levels are in fact overexpressed in the serum of cancer patients. Nevertheless, the findings of Leong et al (2004) should not be called into question, since the ELISA method was not used by those authors. Recently, Mapes et al (2018) have developed a non-transformed mammary epithelial cell-line overexpressing CUZD1 and demonstrated that CUZD1 overexpression increased cell proliferation. In addition, when these cells were injected orthotopically into the mammary gland they had the ability to form adenocarcinomas. Taken together, these results suggest that CUZD1 may have a role in human breast tumorigenesis.

Molecular analysis of the *Deleted in Malignant Brain-Tumor-1* (DMBT1) gene, through representational differential analysis, was performed by Somerville et al (1998). Deletions of the DMBT1 gene were found in prostate cancer (Leube et al., 2002). In this work, loss of heterozygosity (LOH) was analyzed using microsatellite markers for the 10q23-26 and 8p chromosomal regions in 59 prostate cancer samples with different tumor grades. Loss of the DMBT1-containing region was found in seven tumors and deletions in the 10q23-26 region were more frequent in tumors of higher grade and stage, which may indicate that loss of 10q is a late event in the carcinogenesis of these tumors.

Endoglin is also a ZP-domain protein with a powerful association with cancer. Endoglin, also known as Cluster of Differentiation Molecule-105 (CD105), is expressed in the endothelial cells, with particular expression on peri- and intratumoral blood vessels, reason why it had been used as a marker of tumor associated angiogenesis (Burrows et al., 1995; Fonsatti et al., 2001; Fonsatti et al., 2003; Nassiri et al., 2011). Quantification of endoglin expression by immunohistochemistry can be used as a prognosis marker since high levels of expression are associated with more aggressive tumors. Likewise, high levels of the soluble form of endoglin can be detected at the

plasma of patients with solid and hematological tumors and its quantification can work as a diagnosis marker (Takahashi et al., 2001; Calabrò et al., 2003). Besides, it would also be interesting to make use of these discoveries to assess therapy response.

Endoglin can modulate the response to transforming growth factor beta 1 (TGF-β1) given the findings of Li et al (2000), in which the suppression of CD105 promotes TGF-β1-induced growth and migration suppression. In contrast, decreased expression of endoglin on prostate cancer cells was associated with metastasis proneness since endoglin was found to be associated with focal adhesion complexes and its loss can result on more detached and motile cells (Liu et al., 2002). Further studies are required to clarify endoglin role on cell adhesion and invasion.

Given its almost exclusive expression in the tumor vasculature, anti-endoglin therapies have been developed to inhibit metastasis and promote tumor shrinkage with promising results (for review see: Rosen et al., 2014). However, like other therapies based on antibodies, there are no perfect target. This lack of specificity and the high probability of side effects lead to some apprehension by clinicians (Balza et al., 2001; Seon, 2002).

Expression of the *Placenta-specific-1* (PLAC1) gene has been demonstrated in a variety of cancer types including breast, prostate and ovarian cancer (for review see: Fant et al., 2010). Recently, PLAC1 expression was evaluated by immunohistochemistry in the study of Ghods et al (2014). Authors showed that PLAC1 expression levels increased throughout tumor progression (normal tissue < benign prostate hyperplasia < high-grade prostatic intraepithelial neoplasia < prostate cancer) and the highest expression was observed in poorly differentiated cells. These observations suggested that PLAC1 expression is an early event in prostate carcinogenesis and that PLAC1 can be a novel target for immunotherapy, mainly in patients in more advanced stages of cancer.

PLAC1 expression in normal tissue is rare and thus this protein is a potential target for cancer immunotherapy. However, PLAC1 expression is also found in the placental tissue, leading us to questioning the possible effect of this therapy in female fertility. Liso et al (2017) performed a preliminary study in mice to evaluate if the immunization with PLAC1 peptides affected the fertility of females. Authors inoculated female mice with the PLAC1 peptide to promote an immune response and the production of anti-PLAC1 antibodies. They demonstrated that vaccination against PLAC1 did not cause infertility since inoculated females got pregnant and gave birth to normal puppets.

In humans, breast cancer cell-lines were used to evaluate the therapeutic potential of PLAC1-specific T lymphocytes (Li et al., 2018). Authors generate cytotoxic T-lymphocytes against PLAC1 peptides and co-cultured them with PLAC1-expressing breast cancer cell-lines. Cancer cells expressing PLAC1 were specifically identified and eliminated by the activated cytotoxic CD8+ T-cells. Authors also performed an in vivo assay using a breast cancer model of female nude mice where PLAC1 T-cell receptor (TCR)-transduced CD8+ T-cells were transplanted

intravenously through the tail vein. In this assay it was observed that PLAC1 TCR-transduced CD8+ T cells delayed tumor growth when compared with the control group.

1.6. Final remarks

The current medicine is governed by the principle of prevention with early diagnosis and appropriate therapy being the foremost contributors for human wellbeing. Recent studies have described the role of human ZP glycoproteins on several human disorders. Therefore, new therapeutic strategies using these proteins are promising technologies for future clinical application.

As biomarkers, ZP-domain proteins may result in new biological measurable indicators of: a) oocyte quality and hence lead to increased rates of success in ART treatments; and/or b) cancer and here function as diagnostic, prognostic, predictive or therapeutic tools with high specificity and sensibility since its presence on tumor cells, metastases as well as recurrences.

As autoantigens, ZP-domain proteins are also an exciting therapeutic option both in patients with autoimmune disease and/or cancer. Although this approach has already some promising results in the reduction of autoantibodies titer and disease symptoms in several animal models as well as in cross-breeding contraception, more studies are needed before its human application.

ZP-domain proteins are present in several types of cancer with mutations or an altered expression, a fact that cannot go unnoticed. In some cases, the mutations occur in the ZP-domain, but no causal relationship is given by the authors. However, without further studies to uncover the functions of the ZP-domain, the development of new therapies or biomarkers remain only as a fond hope.

Nevertheless, we believe that the therapeutic potential of the ZP-domain proteins prospects considerable engagement, and hopefully they may in near future be combined with clinical strategies.

II. AIMS

Recent studies have shown an association between the ZP-domain proteins and cancer. One example is the expression of ZP3 protein in prostate and ovarian cancer. Prostate cancer and the cell-line PC3 have been described ultrastructurally but with small detail. For this reason, we proposed to perform a detailed characterization of the ultrastructure of the human prostate cancer cell-line PC3 and correlated it with the already existing information.

The evaluation of the expression of the ZP1-ZP4 proteins in prostate cancer tissue and PC3-cells was also one of the goals of the present work in order to confirm the expression of ZP3 and determine if the remaining ZP glycoproteins, which have not yet been evaluated, were also expressed by the prostate cancer tissue and PC3-cells. Another goal of our work was the evaluation and quantification of the expression of the genes ZP1-ZP4 on both pavement and aggregated PC3-cells and correlated it with the protein expression on both prostate cancer tissue and PC3-cells. Finally, we proposed to investigate the association between the ultrastructural morphology (pavement and aggregated cells) and ZP-proteins expression.

III. RESULTS

Structural and molecular analysis of the cancer prostate cell line PC3: oocyte zona pellucida glycoproteins.

Original article submitted to Tissue and Cell (Attachments)

Structural and molecular analysis of the cancer prostate cell line PC3: oocyte zona pellucida glycoproteins

Jéssica Costa[1], Rute Pereira[1,2], Jorge Oliveira[3], Ângela Alves[1,2], Ângela Magalhães[4], Amaro Frutuoso[5], Carla Leal[6], Nuno Barros[7], Rui Fernandes[8], Márcia Barreiro[6], Alberto Barros[7,9,10], Mário Sousa[1,2], and Rosália Sá[1,2]

[1] Laboratory of Cell Biology, Department of Microscopy, Institute of Biomedical Sciences Abel Salazar (ICBAS), University of Porto (UP), Rua Jorge Viterbo Ferreira, 228, 4050-313 Porto, Portugal; [2] Multidisciplinary Unit for Biomedical Research (UMIB), University of Porto, Rua Jorge Viterbo Ferreira, 228, 4050-313 Porto, Portugal; [3] Center of Medical Genetics Dr. Jacinto de Magalhães (IGM), Hospital Center of Porto (CHP), Praça de Pedro Nunes 88, 4050-106 Porto, Portugal; [4] Department of Pathology, Portuguese Oncology Institute of Porto, Rua Dr. António Bernardino de Almeida, 4200-072 Porto, Portugal; [5] Department of Complementary Means of Diagnosis and Therapy, Service of Pathology, Hospital of Pedro Hispano, Rua Dr. Eduardo Torres, 4464-513 Senhora da Hora, Porto, Portugal; [6] Centre of Assisted Medical Procriation (CPMA), North Maternal Child Center (CMIN), Hospital Center of Porto (CHP), Largo da Maternidade de Júlio Dinis, 4050-651 Porto, Portugal; [7] Centre for Reproductive Genetics A. Barros, Av. do Bessa, 240, 4100-012 Porto, Portugal; [8] Health Research and Innovation Institute (IBMC/i3S), University of Porto, Rua Alfredo Allen, 208, 4200-135, Porto, Portugal; [9] Department of Genetics, Faculty of Medicine, University of Porto, Alameda Prof. Hernâni Monteiro, 4200-319 Porto, Portugal; [10] Health Research and Innovation Institute (IPATIMUP/i3S), University of Porto, Rua Alfredo Allen, 208, 4200-135, Porto, Portugal.

ABSTRACT

The human oocyte zona pellucida (ZP) is made of four glycoproteins, ZP1-ZP4. Recently, the prostate adenocarcinoma and prostate cancer PC3 cell-line were shown to express the human oocyte ZP3 glycoprotein, which was evaluated in a single report submitted to patenting. To further clarify if oocyte zona pellucida glycoproteins are expressed in prostate cancer tissue and PC3-cells, in the present report we evaluated protein expression of the four ZP glycoproteins in normal prostate tissue, prostate adenocarcinoma tissue and PC3-cells, and performed quantitative mRNA expression of the four ZP glycoproteins in the PC3 cell-line. Additionally, as PC3-cells have not yet been studied in detail regarding their ultrastructural characteristics, in the present report we bring forward the detailed ultrastructure of PC3-cells. PC3-cells were divided into pavement and aggregated cells. We observed new ultrastructural features in pavement and aggregated cells, with the later exhibiting two different cell types. In prostate carcinoma tissue and PC3-cells we found protein expression of the four oocyte glycoproteins, ZP1, ZP2, ZP3 and ZP4. Moreover, mRNA expression studies revealed expression of ZP1, ZP3 and ZP4 glycoproteins, but not of ZP2. Interestingly, the mRNA product of ZP1 presents intron retention.

Keywords: Electron Microscopy; Immunocytochemistry; Real Time PCR; Prostate Cancer; PC3 Cell-Line; Zona Pellucida Glycoproteins

1. Introduction

The human oocyte is coated by a translucent network of fine fibrils, the zona pellucida (ZP), which is constituted by four glycoproteins, ZP1, ZP2, ZP3 and ZP4. In the oocyte, ZP1 crosslinks ZP glycoproteins, ensuring ZP integrity; ZP3 is responsible for primary sperm binding; ZP3 and ZP4 induce the sperm acrosome reaction; and ZP2 is responsible for secondary sperm binding and acrosomal vesicle enzyme activation (Lefièvre et al., 2004; Wassarman, 2008; Gupta et al., 2012).

Due to its function in fertilization, ZP3 was investigated as a potential contraceptive through antibody-mediated disruption of sperm-oocyte binding, but this approach was forsaken as results showed that it also elicited ovarian pathology (Gupta et al., 1997; Hasegawa et al., 2014).

The human oocyte ZP3 has likewise been found to be expressed in somatic cells (The Human Protein Atlas, 2018). Based on these observations and due to its immune properties, ZP3 was also investigated in cancer treatments as a protein useful in cancer immunization. In this setting, as ZP3 expression was observed in human granulosa cell tumors and human surface ovarian tumors, authors developed a novel treatment based on immunization against recombinant human ZP3 (Rahman et al., 2012). More recently, the prostate adenocarcinoma and its cell-line PC3 were also shown to express ZP3, and authors are currently developing a ZP3-based immunotherapy against prostate adenocarcinoma, with data submitted to patenting (Bennink, 2016)

In the Human Protein Atlas (HPA: online version 18; last acceded at 14th June of 2018), protein and mRNA expression of several genes is organized according to normal tissue, cancer tissue and different cell-lines. Regarding ZP1, data for protein expression was not available and mRNA expression was found in certain normal tissues (excluding prostate), in certain cancer tissues (including prostate) and in certain cancer cell-lines (excluding PC3). ZP2 protein expression was found in certain normal tissues (excluding prostate) an in certain cancer tissues (including prostate), whereas mRNA expression was observed in certain normal tissues (excluding prostate) and in certain cancer cell-lines (excluding PC3) and was not expressed in cancer tissues. ZP3 protein expression was found in certain normal tissues (excluding prostate) and was not expressed in cancer tissues, whereas mRNA expression was observed in all normal tissues (including prostate), cancer tissues (including prostate) and cancer cell-lines (including PC3). ZP4 protein expression was found in certain normal tissues (excluding prostate) and was not expressed in cancer tissues, whereas mRNA expression was observed in certain normal tissues (excluding prostate) and in certain cancer cell-lines (excluding PC3) and was not expressed in cancer tissues.

Thus, according to HPA, prostate cancer was shown to express protein ZP2 and to express ZP1 and ZP3 mRNA, whereas in the PC3 cell-line only ZP3 mRNA expression was found. In a previous work using prostate tissue and ZP3 expression (Bennink, 2016), authors also did not find ZP3 protein expression in normal prostate tissue, but observed, contrary to HPA, protein

cytoplasmic expression in prostate cancer tissue; in relation to mRNA expression, authors also observed ZP3 expression in prostate cancer but not, contrarily to HPA, in normal prostate tissue. Regarding the PC3 cell-line, authors observed ZP3 cytoplasmic protein expression and mRNA expression.

In the study of prostate cancer, 21 cell-lines have been described but only three of them are routinely used, namely PC3, LNCaP and DU145 (van Bokhoven et al., 2003; Tai et al., 2011). The PC3 cell-line is derived from a bone metastasis of a grade IV prostate adenocarcinoma, LNCaP is derived from a left supraclavicular lymph node metastasis and DU145 is originated from a brain metastasis. Of the prostate cancer cell-lines, ZP3 glycoprotein expression was only found in PC3-cells, which was evaluated in a single report submitted to patenting (Bennink, 2016). This is the reason why we choose the PC3 cell-line to evaluate oocyte ZP glycoprotein expression. To further clarify if ZP glycoproteins are expressed in prostate cancer tissue and PC3-cells, in the present report we evaluated protein expression of the four ZP glycoproteins in normal prostate tissue, prostate adenocarcinoma tissue and PC3-cells, and performed quantitative mRNA expression of the four ZP glycoproteins in the PC3 cell-line. Additionally, as PC3-cells have not yet been studied in detail regarding their ultrastructural characteristics, with previous authors presenting the description of only a single cell (Ravenna et al., 1996; Kim et al., 2005; You et al., 2015; Xu et al., 2016) or some cellular details (Kaighn et al., 1979), in the present report we bring forward the detailed ultrastructure of PC3-cells.

2. Materials and methods

2.1. Ethics

Ethical guidelines were followed in the conduct of research, with informed consent having been obtained before the beginning of the present work. This work did not involve human or animal experiments. An approval by an Ethics Committee and the provisions of the Declaration of Helsinki as revised in Tokyo 2004 on human experimentation does not apply to this kind of work. Paraffin tissue blocks were provided under informed consent for the use of this kind material for hospital diagnostic and research purposes. According to the National Law on Medically Assisted Procreation (http://data.dre.pt/eli/diario/1/142/2017/0/pt/html) and the National Council on Medically Assisted Procreation guidelines (http://www.cnpma.org.pt/Docs/Profissionais_Requisitos_CentrosPMA.pdf), surplus donated oocytes were used under patient informed consent from cases enrolled in infertility treatments, with no further authorizations being required.

2.2. Cell culture

The human PC3 cell-line was kindly provided by Prof. Ragnhild A. Lothe from the Department of Cancer Prevention at the Institute for Cancer Research, Oslo, Norway. The PC3 cell-line is derived from a prostate carcinoma and were maintained in culture flasks of 25cm2 (Sarstedt, Nümbrecht, Germany) in Roswell Park Memorial Institute (RPMI)-1640 medium (Merck, Darmstadt, Germany) supplemented with 10% Fetal Bovine Serum (FBS; Merck) and 1% of penicillin-streptomycin (Merck) at 37ºC, 5% CO2. The medium was then replaced with RPMI serum-free medium to starve cells and improve anchorage-independent grow. After 24h, cells were trypsinized with TripLETM Express (Gibco, Thermo Fisher Scientific, Waltham, Massachusetts, USA) and centrifuged at 1200 rpm for 5 min. The cell pellet was resuspended in RPMI serum containing medium and used for Transmission Electron Microscopy (TEM), histochemistry, immunohistochemistry (IH), immunocytochemistry (IC) and molecular biology studies.

For TEM, cell suspensions were used in two systems. In the first, the PC3 cell line was cultured in In Vitro Fertilization (IVF) Petri dishes (35 mm; Nunc, Roskild, Denmark) for three days on a microdrop of RPMI medium under liquid paraffin (Origio, Malov, Denmark) to improve anchorage-independent growth (by decreasing the adhesion area). The aggregates of PC3-cells that grew in suspension (aggregated-cells) were aspirated and processed for TEM. The other system used the four well Lab-Tek Chamber Slide System (Electron Microscopy Sciences, Hatfield, Pennsylvania, USA). In this case, PC3-cells were cultured on wells and left to grow until total confluence. When aggregates were observed in suspension, the medium (along with the cell aggregates) were removed and the cells that grew adherent to the bottom of the well (pavement-cells) were submitted to TEM processing on the same well.

Concerning IC and molecular biology studies, the PC3 cell-line was maintained on a new culture flask with RPMI serum containing-medium were cells grew until total confluence. By this time (3 days), the culture medium was replaced and culture left till the end of the experiment (6 days) to preserve the aggregates that grew in suspension. After more three days, cell aggregates were well established and could be observed in the inverted microscope (CkX41; Olympus, Tokyo, Japan). At this point, the culture medium was aspirated along with cell aggregates and placed on a Cellstar tube (Greiner Bio-One, Frickenhausen, Germany). Cells that grew adherent were trypsinized and placed on another Cellstar tube. Both tubes were centrifuged at 1200 rpm (5 min). The supernatant was discharged and the pellet resuspended in RPMI medium. Half of the resulting suspension was used to make cell smears for IC and the remaining cell suspension was used for RNA extraction.

2.3. Transmission electron microscopy

PC3-cells were processed for TEM according to a previously published protocol (Sá et al., 2011; Sousa et al., 2015). Aggregates of PC3-cells that grew in suspension were aspirated and fixed with Karnovsky [2.5% glutaraldehyde (Merck) plus 4% paraformaldehyde (Merck) in 0.15M sodium cacodylate buffer, pH 7.3 (BDH, Poole, UK)] for 2h at room temperature (RT), washed in buffer, post-fixed with 2% osmium tetraoxide (Merck) in buffer containing 0.8% potassium ferricyanide (Merck) for 2h (4ºC), washed in buffer (10 min), serially dehydrated in ethanol (Panreac, Barcelona, Spain), equilibrated with propylene oxide (Merck), and embedded in Epon (Sigma-Aldrich, Steinheim, Germany).

Pavement-cells processing was performed directly in the wells of the Lab-Tek Chamber Slide System. Fixation was performed with 8% glutaraldehyde plus 4% paraformaldehyde (1h; RT) followed by 4% glutaraldehyde plus 2% paraformaldehyde (overnight; 4ºC) in buffer. After washing with 0.15M sodium cacodylate buffer, post-fixation was accomplished with osmium tetraoxide for 2h (4ºC). Afterwards, pavement-cells were washed in buffer (15 min), incubated with 1% aqueous uranyl acetate (30 min; BDH), washed in distilled water (15 min), serially dehydrated in ethanol, equilibrated with propylene oxide/Epon with continuous stirring, and embedded in Epon. Semithin and ultrathin sections for both aggregated-cells and pavement-cells were made with a diamond knife (Diatome, Hatfield, Switzerland) in an ultramicrotome (LKB; Leica Microsystems, Weltzlar, Germany). Semithin sections with 2 µm thickness were stained (1% methylene blue in 1% borax aqueous solution plus 1% Azur II in aqueous solution, 1:1; Merck) and observed in a light microscope (BX41; Olympus) to obtain the overall morphology of PC3-cells and select the area of interest. Ultrathin sections were collected on 300-mesh copper grids (Taab, Berks, UK), contrasted with 3% aqueous uranyl acetate (20 min) and Reynolds lead citrate (10 min; Merck), and observed in a transmission electron microscope operated at 60 kV (Jeol 100CXII; JEOL, Tokyo, Japan).

2.4. Histochemistry in semithin sections

For Periodic Acid Schiff (PAS) polysaccharides staining, semithin sections of 2 µm were collected in adhesive slides (Starfrost, Knitttel-Glass, Brunswick, Germany) and dried for 2h (60ºC). Removal of the Epon resin from semithin sections was then performed to facilitate stain penetration. For this, slides were dipped in sodium ethoxy solution (saturated solution of sodium hydroxide in absolute ethanol; Merck) for 10 min (RT), washed twice in absolute ethanol (1 min each; RT) and then in distilled water (3 min; RT). For the PAS reaction, slides were dived in 1% periodic acid solution in water (Merck) for 15 m (RT), rinsed in distilled water (3 min; RT), incubated in Schiff reagent (Merck) for 20 min (RT), under light protection, washed in distilled water (3 min; RT), air-dried and mounted in CoverQuick 2000 medium (VWR, Fontenay-sous-Bois, France). Slides were observed in the light microscope.

For Sudan Black lipids staining, semithin sections of 2 µm were collected in adhesive slides and dried for 2h (60ºC). Oxidation of the reduced osmium from semithin sections was then performed to unblock chemical reactions. For this, slides were dipped in 0.06% hydrogen peroxide solution (Merck) for 10 min (RT) and washed twice in distilled water (3 min; RT). For the Sudan Black reaction, slides were dived in saturated solution of Sudan black in 70% ethanol (Merck) for 15 min (RT), washed twice with 70% ethanol and rinsed with distilled water (3 min; RT). The slides were air-dried and mounted in CoverQuick. Slides were observed in the light microscope.

2.5. Immunohistochemistry

Ovary, prostate and prostate cancer human tissues were analysed from formalin-fixed paraffin-embedded blocks using primary monoclonal antibodies against human ZP1, ZP2, ZP3 and ZP4 (ZP1: sc-365435; ZP2: sc-390422; ZP3: sc-398359; ZP4: sc-49587; Santa Cruz Biotechnology, Santa Cruz, California). Normal ovary tissue was used as a positive control. Immunohistochemistry was performed in tissue sections of 3µm thickness attached to adhesive slides. Tissue sections were deparaffinised with xylene (VWR) and serially hydrated in a decreasing scale of ethanol followed by a wash in distilled water. Heat antigen retrieval was performed with citrate buffer pH 6 (0.1M citric acid plus 0.1M sodium citrate; Merck) in a microwave (at 600W) for 20 min. Tissue sections were washed in tap water (5 min) followed by distilled water (5 min). Endogenous peroxidases were inhibited with 3% of hydrogen peroxide (Merck) and non-specific background staining was minimized with normal horse serum (Vector Laboratories, Burlingame, California), with both treatments being performed for 30 min.

Sections were incubated with primary monoclonal antibodies for 60 min. For each experiment, a negative control was included, which consisted in the omission of the primary antibody and its replacement by Phosphate Buffer Saline (PBS; Panreac). Ultraview universal diaminobenzidine (DAB) anti-mouse detection kit (Ventana Medical Systems, Tucson, Arizona, USA) was used to reveal expression of ZP1, ZP2 and ZP3 antigens. The ZP4 antigen was revealed using the Vectastain Universal anti-goat Quick Kit (Vector Laboratories). Between each step a wash in three changes of PBS was carried out. After dehydration, sections were mounted on Coverquick. Results were observed in the light microscope. Experiences were performed in triplicate.

2.6. Immunocytochemistry

Donor surplus human oocytes (used as a positive control) were transferred to adhesive slides. PC3-cell smears were made from cell suspensions containing either pavement-cells or aggregated-cells. Oocytes and PC3-cells were fixed with 1% paraformaldehyde in PBS for 10 min (RT), followed by a wash in three changes of PBS. For permeabilization, cells were incubated in 0.1% Triton X-100 (Sigma) plus 0.1% sodium citrate in PBS for 3 min (4ºC). Cells were then

washed three times in PBS and incubated with 5% Bovine Serum Albumin (BSA; Sigma) for 20 min (RT) to inhibit non-specific binding. After rinsing with PBS, cells were incubated with primary monoclonal antibodies for 1h (37ºC). For each experiment, a negative control was included, which consisted in the omission of the primary antibody and its replacement by PBS. Antibody solution was then removed and a wash of three changes of PBS was performed. Secondary antibody conjugated with fluorescein isothiocyanate (FITC; Santa Cruz Biotechnology) was applied to cells for 45 min (RT). For ZP1, ZP2 and ZP3 we used the secondary antibody anti-mouse FITC (sc-516140), whereas for ZP4 we used the secondary antibody anti-goat FITC (sc-2024). After washing thrice in PBS, PC3-cells were counterstained with Vectashield mounting medium containing 4', 6-diamidino-2-phenylindole (DAPI; Vector Laboratories). Oocytes were washed in PBS but not counterstained with DAPI and observed in PBS. Results were observed in an epifluorescence microscope (Eclipse E400; Nikon, Tokyo, Japan). Experiences were performed in triplicate.

2.7. Molecular biology

2.7.1. RNA purification

Total ribonucleic acid (RNA) from both oocytes and PC3-cells was extracted using column-based methods. Total RNA from PC3-cells was extracted using the PerfectPure RNA Cell & Tissue Kit (5 PRIME, Hamburg, Germany), according to manufacturer instructions. Due to the low number of available oocytes, total RNA from 4 oocytes was extracted using the Single Cell RNA Purification Kit (Norgen, Thorold, Canada), also following the manufacturer instructions. The concentration and purity of RNA samples were determined on a Nanodrop spectrophotometer (ND-1000, version 3.3; LifeTechnologies, California, USA). Only samples with an A260/A280 ratio between 1.8-2.1 were selected as it is an indicative of highly purified RNA.

2.7.2. cDNA synthesis

PC3-cell RNA was converted to complementary deoxyribonucleic acid (cDNA) using the High Capacity cDNA Reverse Transcription kit (Applied Biosystems, California, USA), according to manufacturer instructions and including the optional step of "DNase treatment" that is intended to digest genomic DNA (gDNA) to avoid gDNA contamination. For oocytes, RNA conversion was performed with Superscript IV VILO Master Mix (Invitrogen, ThermoFisher Scientific), as per manufacturer instructions, including too the optional step of "DNase treatment", because this enzyme is known to have superior sensitivity and effectivity, even with samples of low RNA concentration, as is the oocytes case.

2.7.3. Primer design

ZP1 (NM_207341.3), ZP2 (NM_003460.2), ZP3 (NM_001110354.1) and ZP4 (NM_021186.4) mRNA sequences were retrieved using the National Center for Biotechnology Information (NCBI) genome browser (http://www.ncbi.nlm.nih.gov/). Primer design was performed using the Primer-BLAST tool (Ye et al., 2012) from NCBI browser using the following parameters: PCR product size from 70bp-250bp; primer melting temperatures from 56ºC-65ºC; and primers must span an exon-exon junction. Each primer pair was followed tested against the presence of dimers using the FastPCR software (v. 3.7.7; Institute of Biotechnology, University of Helsinki, Finland) applying a cut-off dimer local alignment similarity of 72%. Moreover, the Primer-BLAST tool (Ye et al., 2012) was used to evaluate the specificity towards the regions of interest. The resulting primer sequences (5'->3') are described on **Table 1**.

2.7.4. Polymerase Chain Reaction

ZP1, ZP2, ZP3 and ZP4 genes were amplified by Polymerase Chain Reaction (PCR) using the primers previously design. PCR conditions were optimized using oocyte cDNA as control. Final conditions used to amplify the referred genes were the following: an initial denaturation for 10 min (95ºC), followed by 38 cycles of denaturation for 30 sec (95ºC), primer annealing for 30 sec at specific annealing temperature (**Table 1**), and extension for 60 sec (72ºC). A final extension was performed for 8 min (72ºC), followed by a gradual decrease of temperature till 4ºC. The PCR reaction mixture (20 µl) contained: 10 µL of AmpliTaq Gold 360 Master Mix (ThermoFisher Scientific), 1 µL of each primer (at 10 pmol/µL) (NZYTech, Lisbon, Portugal), 1 µL of cDNA and 7 µL of sterile bidistilled water. For ZP4, the PCR reaction master mix was replaced by the PCR 2x Master Mix (Promega, Madison, USA). PCR reactions were conducted in a thermocycler (VERITI; LifeTechnologies).

Table 1: Designed primers for each gene, their annealing temperature after optimization and the expected length for each amplification product.

Gene	Primers	Product length (base pairs, bp)	Annealing Temperature
ZP1 NM_207341.3	F: CATTCAGGCATCCATTTTCC R: ACGAGCTGAAGGTCTCGTCT	104bp	60ºC
ZP2 NM_003460.2	F: GCCAGAAGGATTTCATGTCTTT R: GCACCATCACCAACCTCAA	112bp	58ºC
ZP3 NM_001110354.1	F: GGTTGTTTGTGGACCACTGC R: TCGACAAGACAGCCATGGAA	94bp	60ºC
ZP4 NM_021186.4	F: CTTCTAGCCCGAGATGCTCC R: ACGTTCCGAGACACAGCAAT	215bp	58ºC
GAPDH NM_001289745.2	F: AGGTCGGAGTCAACGGATTT R: TGGAATTTGCCATGGGTGGA	157bp	58ºC
EMC7 NM_020154.2	F: ATGAGACGGGAAATGGAGCA R: CCAGTGTTGCCGTGTTTGTG	207 bp	58ºC

PCR products (5 µL) were analyzed by 2% agarose gel electrophoresis: mix of TAE 1X SeaKem LE Agarose (Lonza, Rockland, USA) and 5µL/100ml of GelRed Nucleic Acid Gel Stain, 10,000x in water (Biotium, California, USA). GeneRuler DNA Ladder Mix (ThermoFisher Scientific) was used as a marker for sizing and approximate quantification of cDNA fragments. Finally, the PCR products were visualized and photographed in a Luminescent Image Analyzer (LAS-3000; v. 2.2; Fuji Film, Tokyo, Japan).

2.7.5. Sanger Sequencing reaction

PCR products were enzymatically purified using the Illustra ExoStar kit (GE Healthcare-Buckinghamshire, UK), following manufacturer instruction. Posteriorly, a new asymmetric PCR was prepared based on Sanger sequencing method. For this asymmetric PCR it was used the BigDye Terminator (v. 1.1) Cycle Sequencing Kit (Life Technologies). The asymmetric PCR included: 2 µL of BigDye Terminator, 1.5 µL of primer (at 10 pmol/µL), 2 µL bidistilled water, and 5 µL of the product from Illustra ExoStar purification. These reactions were then purified using a size selection column method Performa DTR (Dye Terminator Removal; EdgeBio, Maryland, USA). In the final step, the obtained products were resolved and analysed by high resolution electrophoresis in a genetic analyzer (3130xl; LifeTechnologies). The Nucleotide BLAST tool (Zhang et al., 2000; Morgulis et al., 2008) was used to access nucleotide sequence similarity between the sequencing data and the transcript of interest.

2.7.6. Quantitative RT-PCR

Real-time quantitative PCR (qPCR) was performed to evaluate mRNA expression of ZP genes in both PC3-cell types and compared from the expression to oocytes. Specific primers were the same previously described (**Table 1**). GAPDH and EMC7 were used as housekeeping genes to normalize gene expression levels (Eisenberg and Levanon, 2013). qPCRs were carried out in a real-time PCR apparatus (CFX96; Bio-Rad, Hercules, USA) and the efficiency of the amplification was determined for all primer sets using serial dilutions of cDNA (1:5; 1:10; 1:15; and 1:20). PCR conditions and reagents concentrations were previously optimized. qPCR amplifications used 1µL of synthesized cDNA in a 20 µL reaction containing 10 µL NZY qPCR Green (NZYTech) and 1µL of each primer (at 5 pmol/µL) for each gene. The cDNA dilutions were adjusted based on RNA concentration (used to cDNA synthesis) to ensure that samples had an equivalent cDNA concentration. Reaction conditions were the following: 10 min denaturation (95ºC), followed by 40 cycles at 95ºC for 30 sec, and a specific annealing temperature for each gene for 30 sec (**Table 1**). For melting curves, the conditions were 95ºC for 60 sec, 55ºC for 30 sec, followed by an increment of 0.5ºC until 95ºC. Samples were run in triplicate in each PCR assay.

2.8. Statistical analysis

Fold variation of gene expression levels was calculated following the mathematical model proposed, using the formula $2^{-\Delta\Delta Ct}$ (Pfaffl, 2001). The non-parametric Kolmogorov-Smirnov test was run in the IBM SPSS Statistics (IBM Corp Released 2015; IBM SPSS Statistics; v. 23.0) to access the differences on ZP1, ZP3 and ZP4 expression levels between cells.

3. Results

3.1. Ultrastructure of the cell line PC3

3.1.1. Pavement-cells

These cells have an elongated appearance and a surface with numerous long microvilli and stereocilia (**Figs. 1, 2**). The nucleus is lobulated and has a regular outline; the nuclear matrix is pale, with a fine fibrilar appearance, and did not present heterochromatin patches (**Fig. 1B**); small reticulated nucleoli (**Fig 1B-inset**) appeared positioned at the center or in contact with the nuclear envelope (**Fig. 1B**). In one pole of the cell (**Fig. 1A**), the surface showed a lower number of microvilli and the cytoplasm contained numerous elongated and ramified mitochondria with moderate-dense matrix and thin pale cristae (**Fig. 1A-inset**); this region also presented an extensive net of rough endoplasmic reticulum (RER) cisternae, numerous secondary lysosomes and pale vesicles (**Fig. 1A**). The other pole of the cell (**Fig. 2A**) exhibited a lacework of complex surface invaginations that entered deep into the cytoplasm and originate a network of multiple

light vesicles of different sizes containing microvilli (**Figs. 2, 3A**); in this region, there were numerous mitochondria with a pale matrix and thin dense cristae (**Figs. 3B, 4A-inset**), light vesicles and RER cisternae, and rare small dictiosomes (**Fig. 3B**), occasional secondary lysosomes (**Fig. 4B**) and multivesicular bodies (**Fig. 4C**), and the centriole (**Fig. 4E**); this region was rich in microvilli and stereocilia (**Fig. 4D**). Cells were joined through tight-junctions (**Fig. 4F**) and desmosomes (**Fig. 4G**). Near these junctions coated vesicles were observed (**Fig. 4G**). Cytoplasmic small granules observed at high density (**Fig. 4A**) were considered ribosomes, as the cytoplasm was not stained for glycogen with the PAS technique (**Fig. 8A**). Secretory vesicles and lipid droplets were not observed. The absence of lipid droplets was confirmed by a negative staining with Sudan black (**Fig. 8C**).

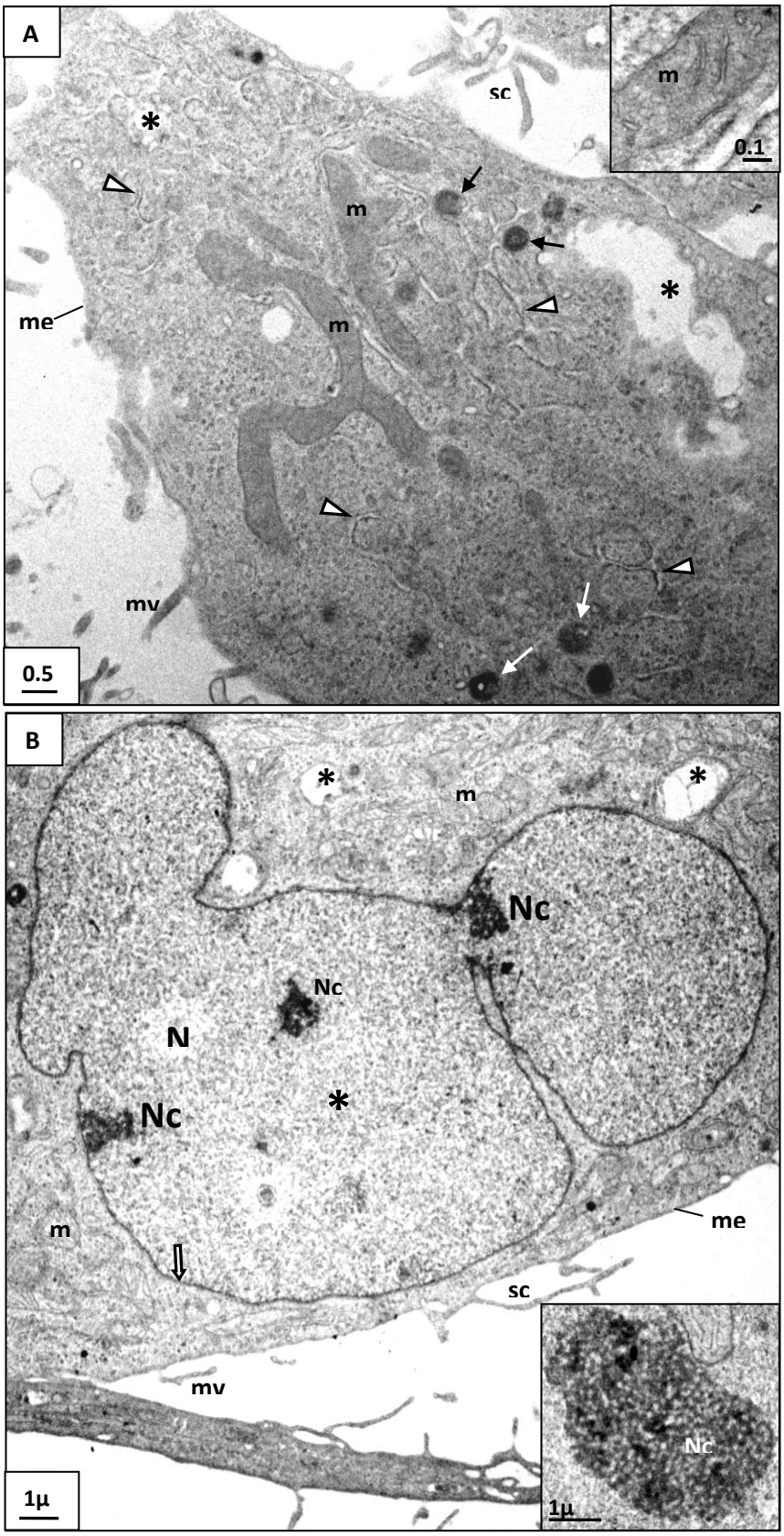

Figure 1. Ultrastructure of PC3 pavement-cells. **A.** In this cell pole, the cytoplasm contains a net of elongated mitochondria (m) that present a dense matrix with thin pale cristae (inset), a net of rough endoplasmic reticulum cisternae (arrowheads), multiple small secondary lysosomes (arrows) and pale vesicles (*). **B**. The nucleus (N) is eccentric, lobulated with a regular outline, and presents a pale matrix (*), without patches of heterochromatin, and with reticulated nucleoli (Nc) (inset). Cell membrane (me); microvilli (mv); stereocilia (sc).

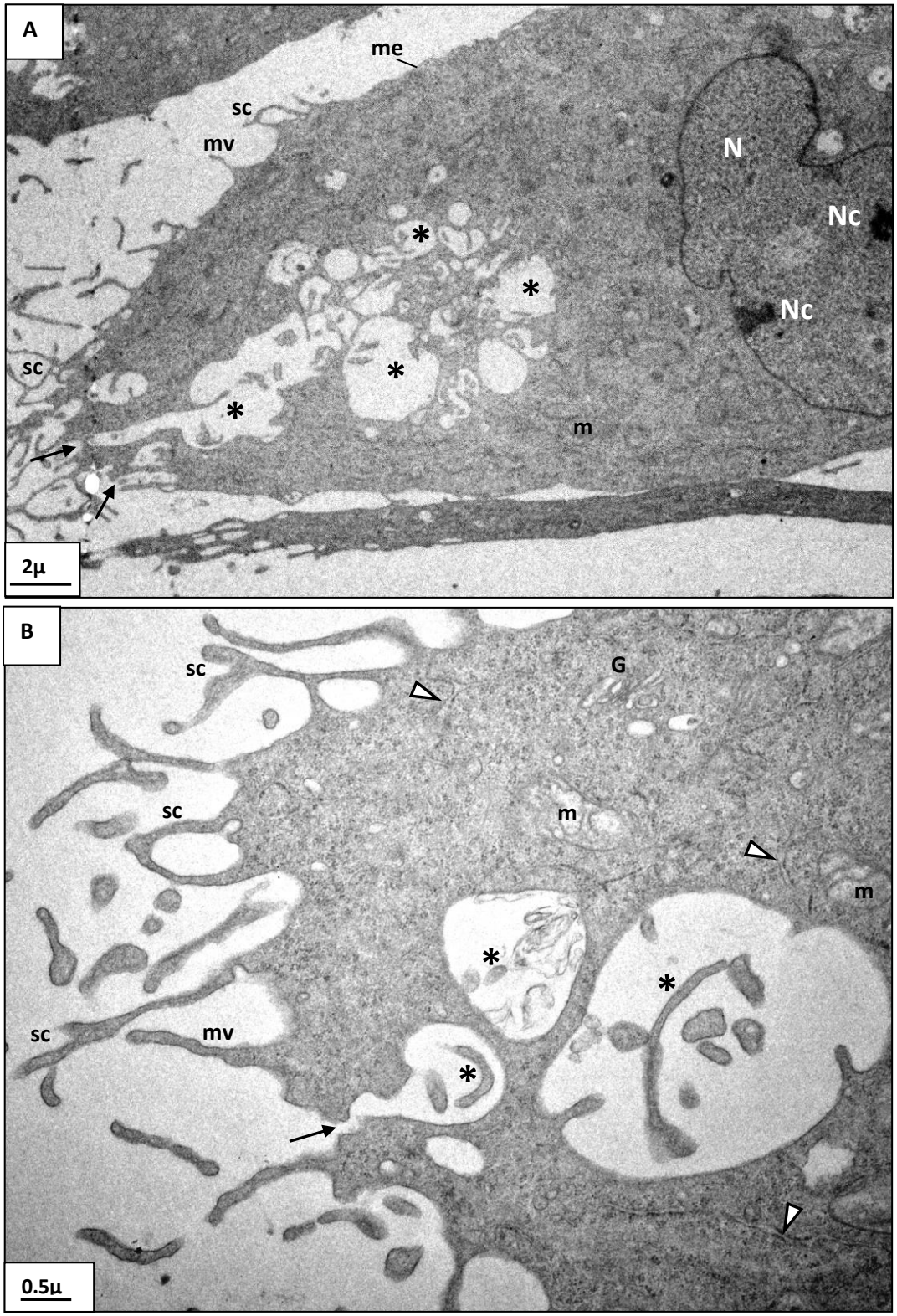

Figure 2. Ultrastructure of PC3 pavement-cells. **A**. In the other pole of the cell, profound surface invaginations (arrows) are observed with appearance of pale vesicles of different sizes with microvilli (*). **B**. Higher magnification to evidence the surface invagination (arrow) originating light vesicles with microvilli (*). Cell membrane (me); microvilli (mv); stereocilia (sc); mitochondria (m); rough endoplasmic reticulum cisternae (arrowheads); dictiosome (G); nucleus (N); nucleoli (Nc).

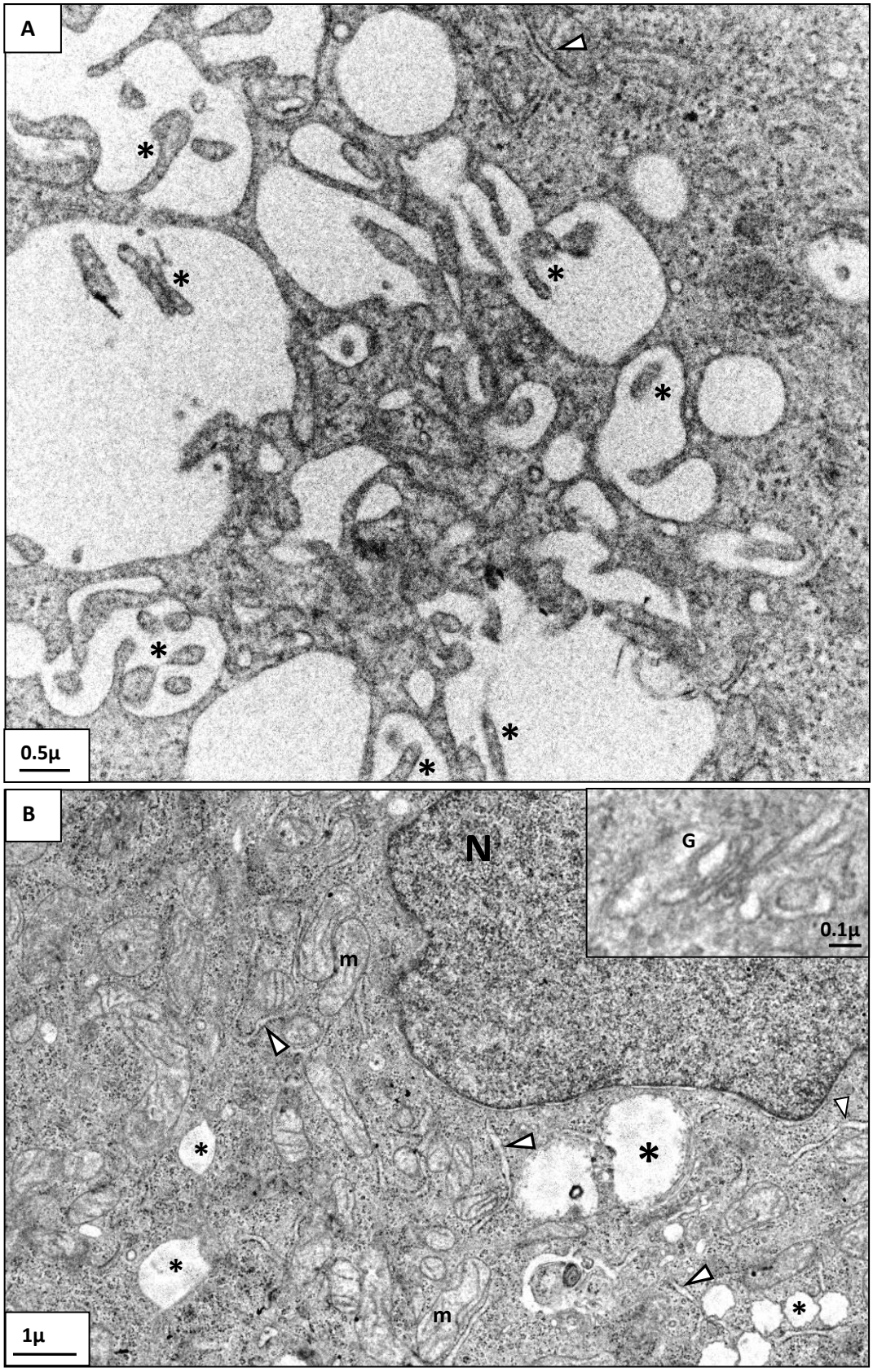

Figure 3. Ultrastructure of PC3 pavement-cells. **A.** Higher magnification to evidence the mesh formed by light vesicles with microvilli (*). **B**. At the pole with surface invaginations, mitochondria (m) are small and present a pale matrix with thin dense cristae. Rough endoplasmic reticulum cisternae (arrowheads); dictiosome (G); vesicles (*); nucleus (N).

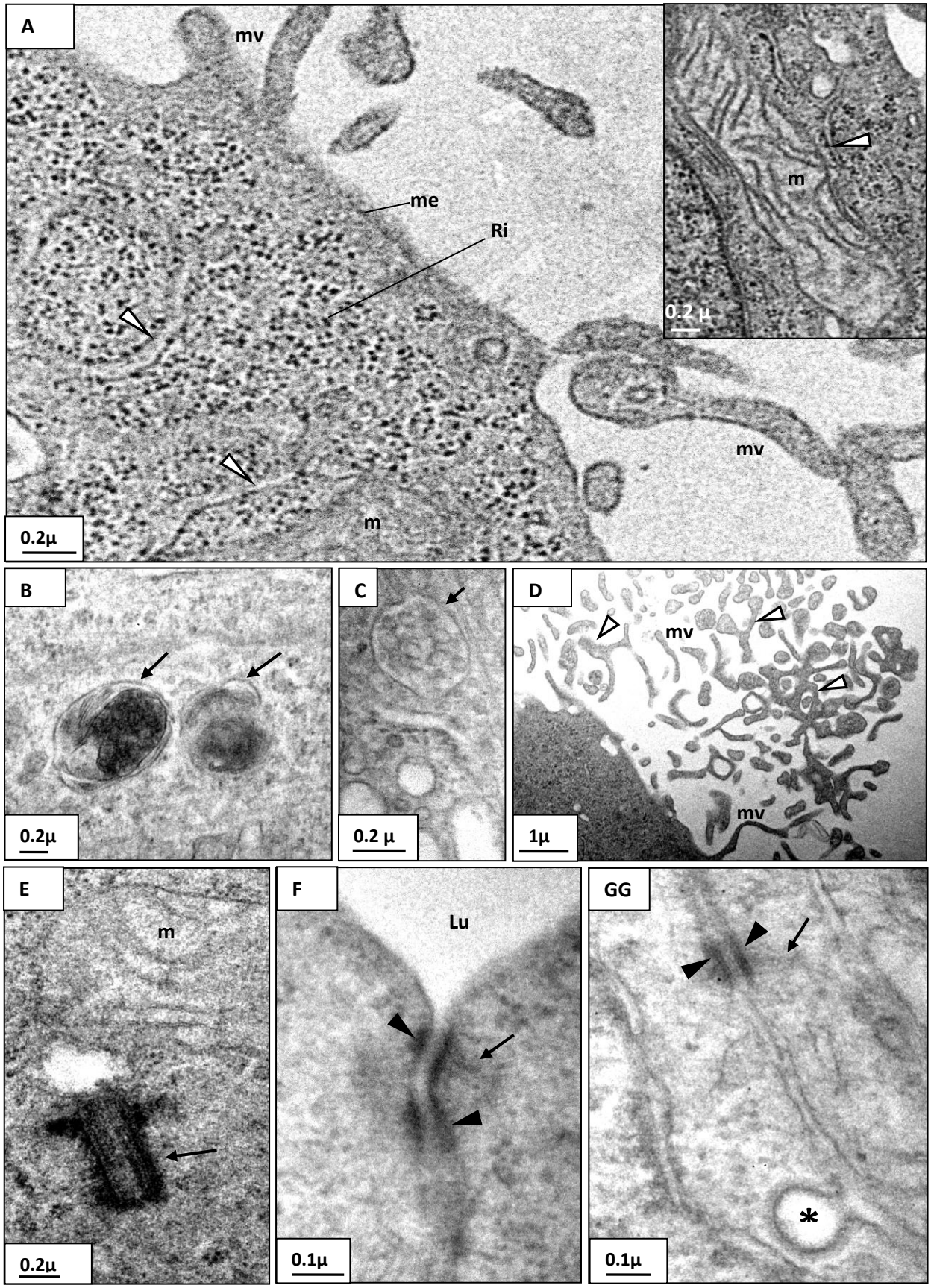

Figure 4. Ultrastructure of PC3 pavement-cells. **A**. Note the richness in free ribosomes (Ri) and the presence of rough endoplasmic reticulum cisternae (arrowheads); mitochondria (m) evidence a pale matrix with thin dense cristae (inset). **B**. Detail of secondary lysosomes (arrows). **C**. Detail of a multivesicular vesicle (arrow). **D**. Detail of the cell surface to show microvilli (mv) and stereocilia (arrowheads), which are branched and anastomosed microvilli. **E**. Detail of the centriole (arrow). **F**. Tight-junction. Note the dense peripheral components (arrowheads) with attached "microfilaments" (arrow). **G**. Desmosome. Note the dense peripheral components (arrowheads) with attached "intermediate filaments" (arrow). Bellow there is a coated vesicle (*), which indicates the presence of receptor-mediated endocytosis. Cell membrane (me); lumen (Lu).

3.1.2. Aggregated-cells

These cells have an oval appearance (**Fig. 5**) and seemed heterogeneous, with presence of two major subtypes: one is rich in lipid droplets (**Fig. 5A**) and the other is rich in membrane invaginations (**Fig. 5B**). The surface of cells presented microvilli and stereocilia and short enlarged microvilli-like protusions (**Figs. 5, 6**); these protrusions established tight junctions between neighboring cells (**Figs. 5B, 5B-upper inset, 6C**). The nucleus was lobulated and had an irregular outline; the nuclear matrix was dense, with a flocculent appearance, and presented internal and peripheral patches of heterochromatin (**Fig. 5**); a large vacuolar nucleolus (**Fig. 5A-inset**) was observed peripherally (**Fig. 5**). The cell-type rich in membrane invaginations presented in one pole complex surface invaginations that entered deep into the cytoplasm, originating multiple light vesicles of different sizes containing microvilli (**Fig. 5B, 5B-bottom inset**). The cell-type rich in lipid droplets presented pale vesicles without evident signs of microvilli (**Fig. 6A**). The cytoplasm of both cell-types contained abundant RER cisternae and mitochondria (**Figs. 5B, 6A, 7**), rare dictiosomes (**Fig. 7a**), a few secretory vesicles (**Fig. 7b**) and secondary lysosomes (**Fig. 7c**), and the centriole (**Fig. 7d**). There were two types of mitochondria: one with a pale matrix and moderate dense longitudinal cristae (**Fig. 7A**) and another with a dense matrix with enlarged pale cristae (**Fig. 7e**). Cells were joined through tight-junctions and desmosomes (**Figs. 5B, 5B-upper inset, 6C, 7B-right inset**). Near these junctions coated vesicles were observed (**Figs. 7B-left inset**). When applied the PAS technique, two types of cells were observed. One cell type was rich in glycogen, whereas the other cell type did not stain (**Fig. 8B**). The same was observed with the Sudan black technique, with one cell type being rich in lipid droplets, whereas the other cell type did not stain (**Fig. 8D**).

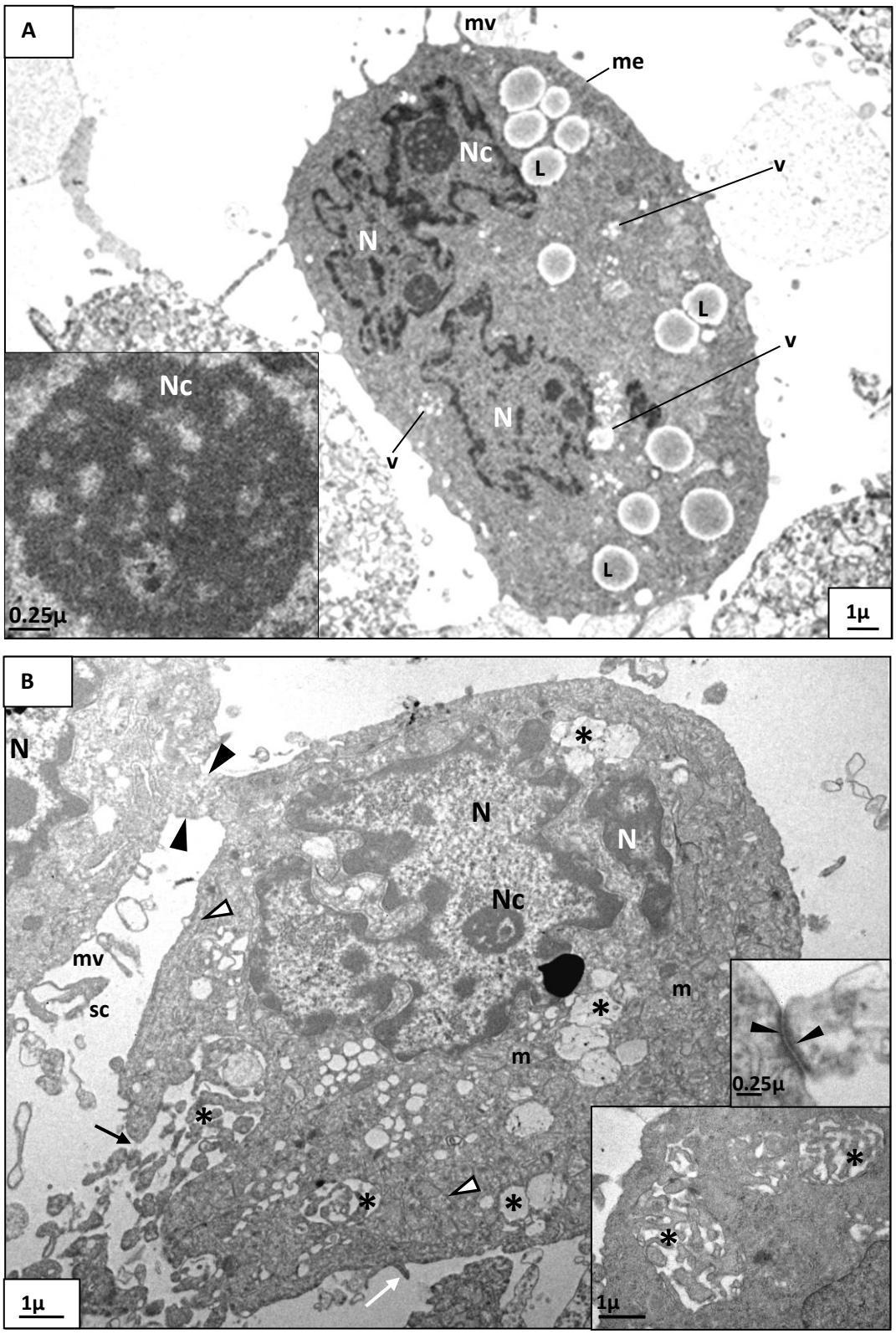

Figure 5. Ultrastructure of PC3 aggregated-cells. **A**. Cell rich in lipid droplets. The nucleus (N) is lobulated, presents an irregular outline, and the nuclear matrix is dense, with patches of heterochromatin and a vacuolar nucleolus (Nc) (inset). The cytoplasm evidences lipid droplets (L) and pale vesicles (v). **B**. Cell with surface invaginations. The nucleus has the same appearance. Profound surface invaginations (arrow) at one pole of the cell originates multiple vesicles with microvilli (*) (bottom inset). The cytoplasm contains mitochondria (m) and rough endoplasmic reticulum cisternae (white arrowheads). Adjacent cells appeared linked by tight-junctions through short surface expansions (black arrowheads) (upper inset). Cell membrane (me); microvilli (mv); stereocilia (sc); short large expansion (white arrow).

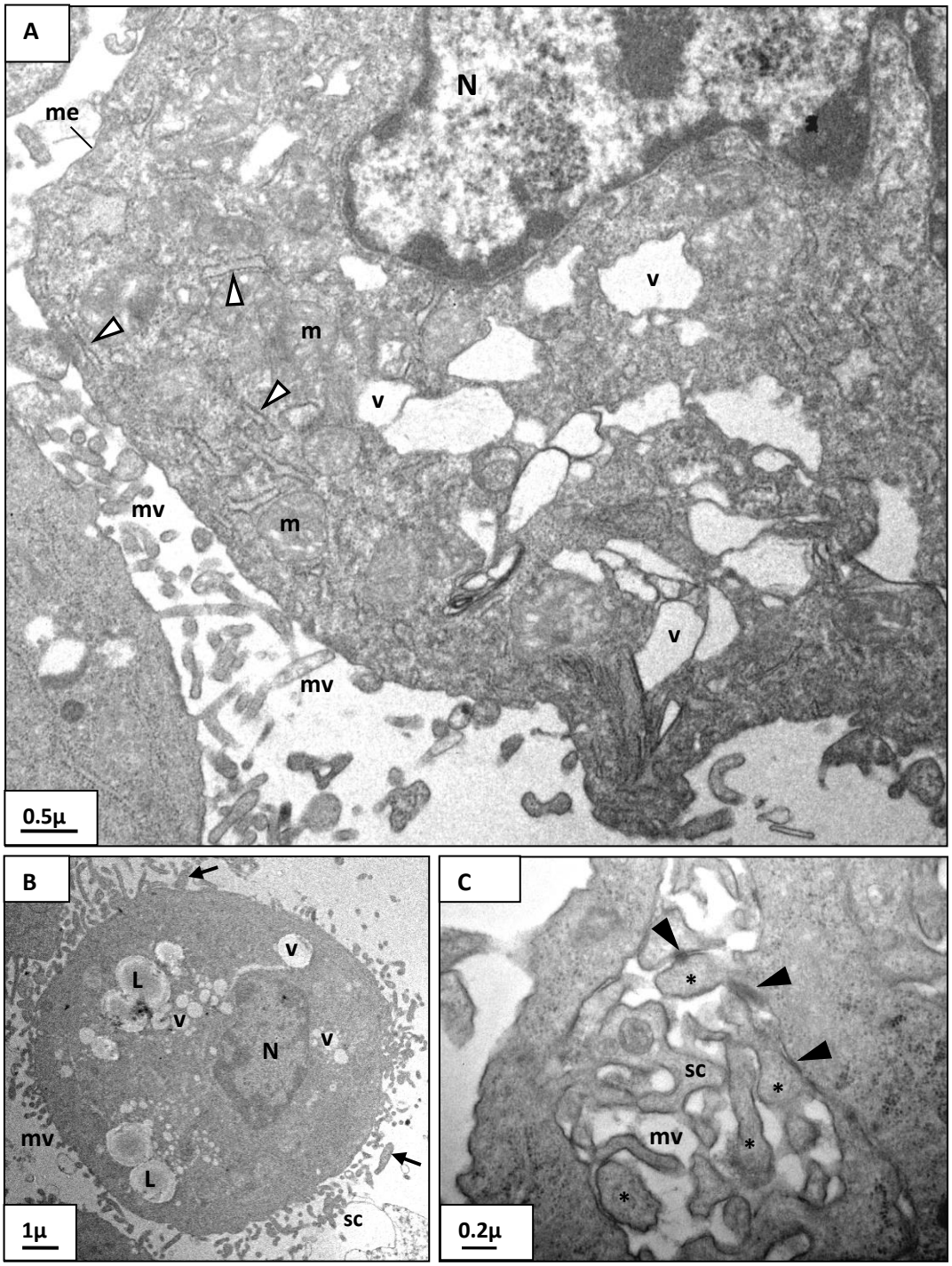

Figure 6. Ultrastructure of PC3 aggregated-cells. **A**. Detail of the cytoplasm a cell rich in lipids. Note the presence of pale vesicles (v) without evident signs of microvilli, mitochondria (m), rough endoplasmic reticulum cisternae (arrowheads) and the nucleus (N). **B**. Low magnification of a cell to show the abundance of lipid droplets (L), microvilli (mv), stereocilia (sc) and short surface expansions (arrows). **C**. Cells appeared linked by tight-junctions (arrowheads) through the short surface expansions (*). Cell membrane (me).

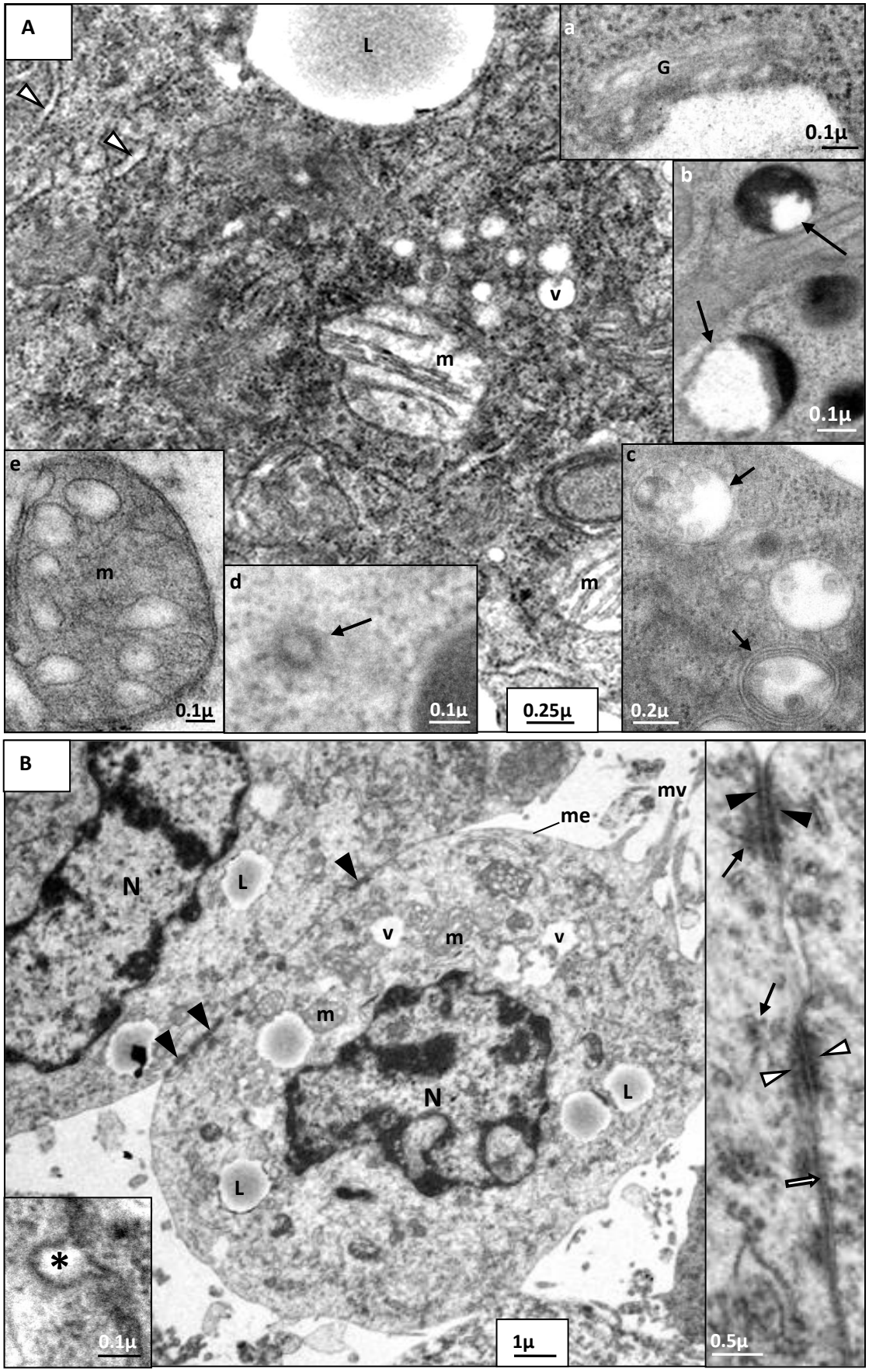

Figure 7. Ultrastructure of PC3 aggregated-cells. **A**. The cytoplasm of cells contains rough endoplasmic reticulum cisternae (arrowheads), dictiosomes (inset a), secretory vesicles (inset b), secondary lysosomes (inset c), the centriole (inset d) and two types of mitochondria, those with a pale matrix and thin dense cristae (m) and other with a dense matrix and enlarged pale cristae (inset e). **B**. Cells joined laterally through tight-junctions (black arrowheads) and desmosomes (right inset: white arrowheads) with their associated filaments (black arrows). Probable gap-junctions could be observed (right inset: white arrow). Near these junctions coated vesicles (*) were observed (left inset). Nucleus (N); lipid droplets (L); vesicles (v); cell membrane (me); microvilli (mv).

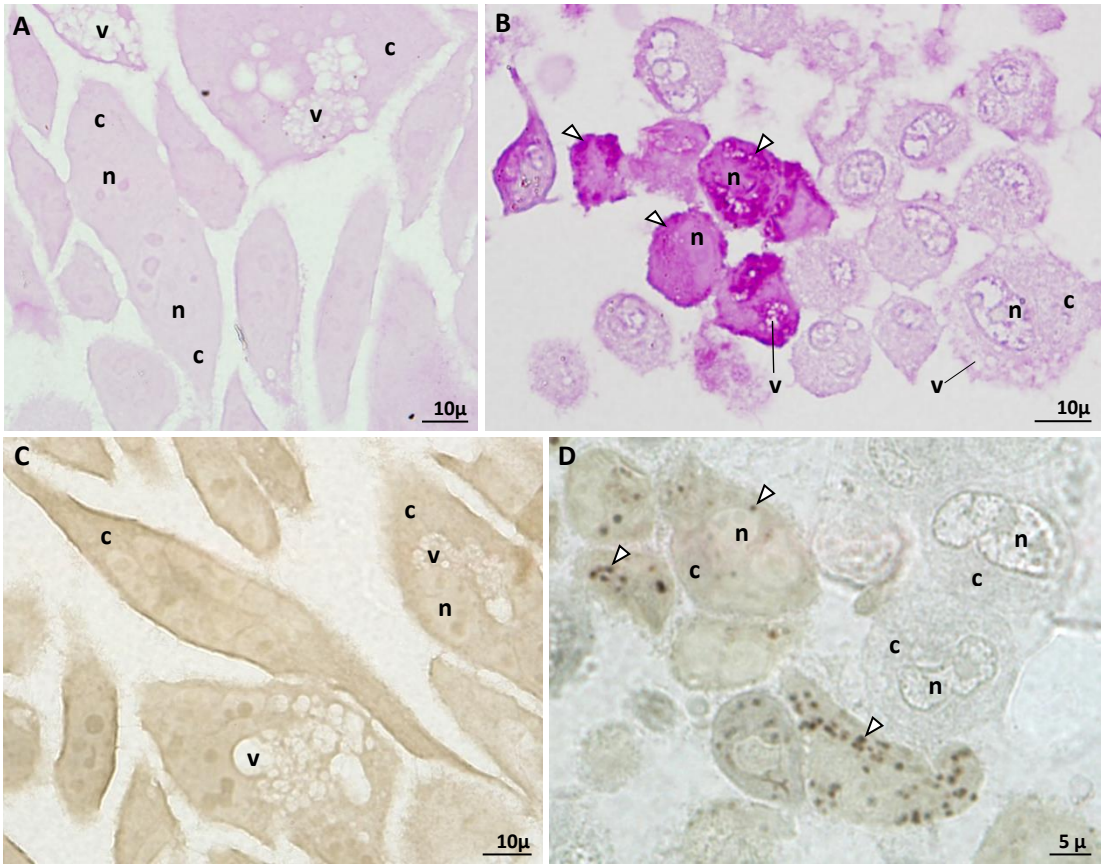

Figure 8. **A, B**. Histochemical detection of glycogen (PAS technique) in PC3 cells. **A**. Pavement-cells stained negative. **B**. Aggregated-cells presented two types of cell staining, one positive (arrowheads) and the other negative. Nucleus (n); cytoplasm (c); vesicles (v). **C, D**. Histochemical detection of lipids (Sudan black technique) in PC3 cells. **C**. Pavement-cells stained negative. **D**. Aggregated-cells presented two types of cell staining, one positive (arrowheads) and the other negative. Nucleus (n); cytoplasm (c); vesicles (v).

3.2. Immunohistochemistry

As expected, ovarian follicles showed a positive staining of the zona pellucida for the four ZP glycoproteins (**Fig. 9A-D**). A relative lower staining intensity of the ZP was observed for glycoproteins ZP2 and ZP4, and a relative higher staining intensity of the ZP was observed for glycoproteins ZP1 and ZP3. A relative strong staining in the ooplasm was observed for glycoprotein ZP4 followed in relative staining intensity by glycoproteins ZP3, ZP1 and ZP2. The normal prostate tissue did not show any staining regarding the four ZP glycoproteins. In the prostate adenocarcinoma tissue, a positive staining for the four ZP glycoproteins was observed in the surface and cytoplasm of the cells (**Fig. 9E-H**). The relative staining intensity was higher for ZP3 and ZP2 and lower for ZP4 and ZP1.

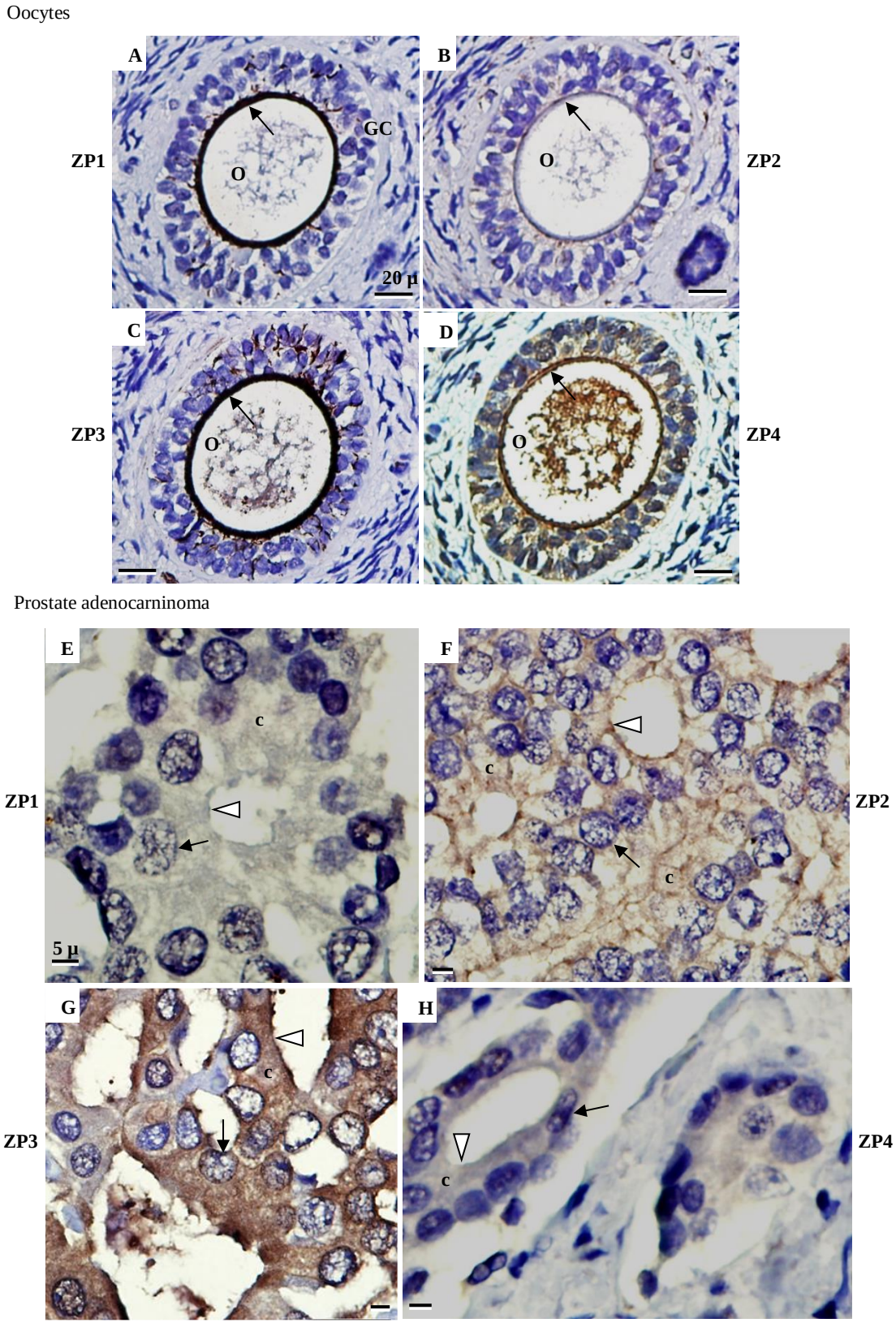

Figure 9. Immunohistochemical detection of zona pellucida glycoproteins ZP1 (**A, E**), ZP2 (**B, F**), ZP3 (**C, G**) and ZP4 (**D, H**). **A-D**. Human oocytes: staining was observed in the zona pellucida (arrows) and in the ooplasm (o). Granulosa cells (GC). Bars: 20 µm. **E-H**. Prostate adenocarcinoma tissue cells: note labeling in the cytoplasm (c) and surface (arrowheads) of the cells. Nuclei (arrows). Bars: 5 µm.

3.3. Immunocytochemistry

As expected, oocytes showed a positive staining of the zona pellucida for the four ZP glycoproteins (**Fig. 10A-D**). A relative strong staining of the ZP was observed for glycoprotein ZP1, followed in relative intensity by glycoproteins ZP4, ZP3 and ZP2. A relative strong staining in the ooplasm was observed for glycoprotein ZP4, followed in relative intensity by glycoproteins ZP3, ZP1 and ZP2. Regarding PC3-cells, both pavement-cells (**Fig. 10E-H**) and aggregated-cells (**Fig. 10I-L**) showed a positive staining for the four ZP glycoproteins in the surface and cytoplasm of the cells, with similar relative intensities.

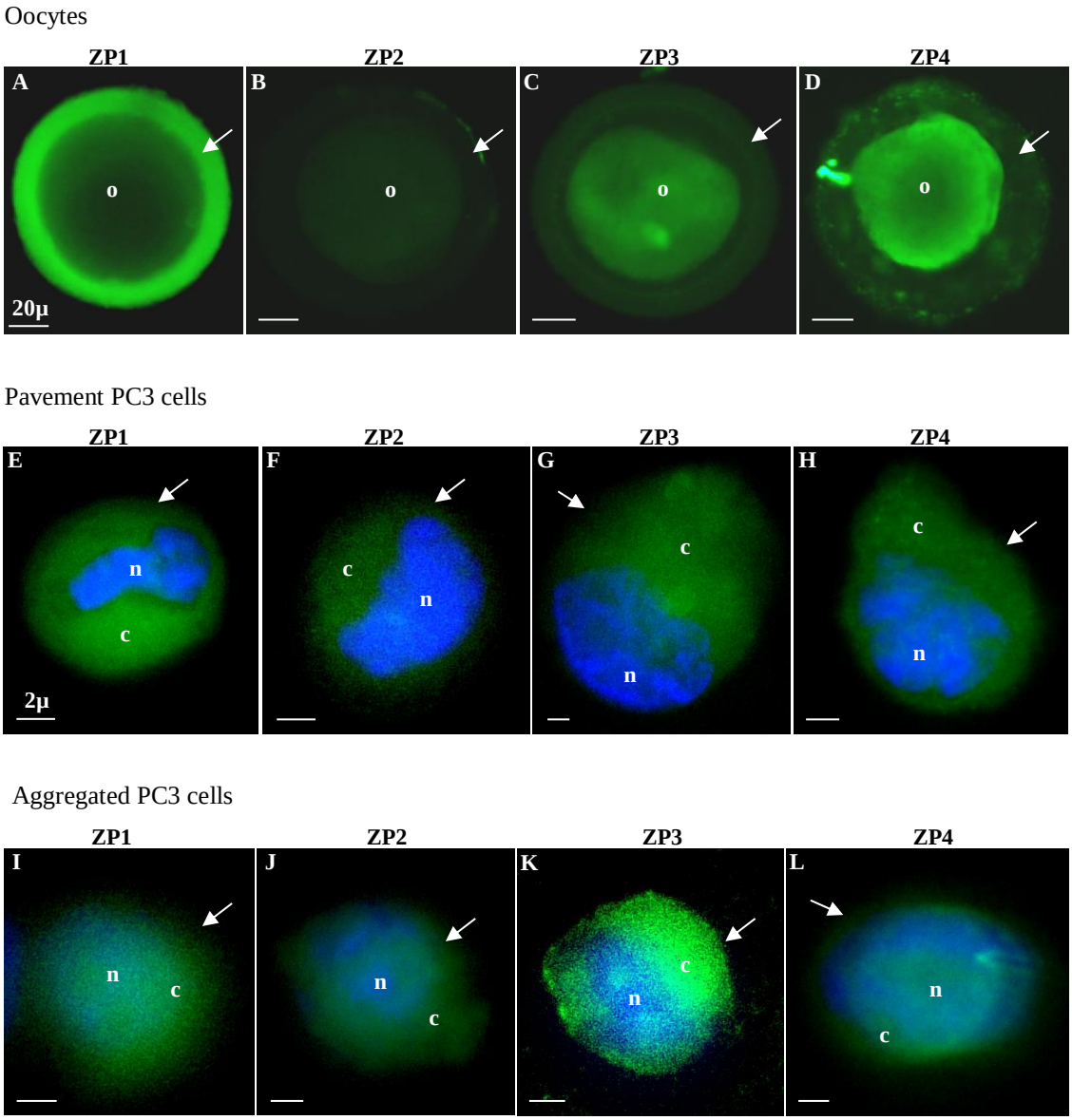

Figure 10. Immunocytochemical detection of zona pellucida glycoproteins ZP1 (**A, E, I**), ZP2 (**B, F, J**), ZP3 (**C, G, K**) and ZP4 (**D, H, L**). **A-D**. Human oocytes: staining was observed in the zona pellucida (arrows) and in the ooplasm (o). Bars: 20 µm. **E-H**. Pavement-cells. **I-L**. Aggregated-cells. in PC3-cells, note labeling in the cytoplasm (c) and cell surface (arrows). Nuclei (n). Bars: 2 µm.

3.4. Molecular biology

Gel electrophoresis (**Fig. 11A**) of PCR amplification products from the positive controls (oocytes) revealed one specific band with the expected size for each interest gene (ZP1, 104bp; ZP2, 112bp; ZP3, 94bp; ZP4, 215bp). Regarding PC3-cells and relative to the ZP1 gene, on both pavement and aggregated cells it was observed one amplification product with a length of approximately 190bp, greater than that observed at the positive control. The result of ZP2 gene amplification in pavement-cells revealed an inconspicuous product with the same length of the control, with no amplification product observed in aggregated-cells. For ZP3 and ZP4, both pavement and aggregated cells revealed an amplification product with the same length of the control sample. Negative controls did not reveal any amplification product.

The specificity of the PCR products was confirmed by Sanger sequencing. All control samples have significant similarity with the transcript of interest (99-100% of identity and query cover and an E-value below $1e^{-6}$). Regarding ZP3 and ZP4, a significant similarity was observed on PCR products from both pavement and aggregated cells. For ZP2, no significant similarity was found for the PCR products of pavement-cells, which means that the PCR product may not correspond to ZP2 or that ZP2 expression is very low to be detected. In relation to ZP1, sequencing of PCR products of both pavement and aggregated cells demonstrated a significant similarity with the transcript of interest with 100% identity and an E-value below $1e^{-6}$ like control samples but with a query cover of 23-26%. A detailed observation of the sequencing result of the PCR products revealed that, for both pavement and aggregated cells, the amplification product of ZP1 corresponded to a transcript variant containing intron 7.

EMC7 was not considered a good housekeeping gene for these cells given its variability. For this reason, relative quantification (qRT-PCR) of the ZP1, ZP3 and ZP4 genes on oocytes and PC3-cells was normalized to the GAPDH reference gene (**Fig. 11B**). Using the normalized values and the oocyte mRNA as reference, the ratio of oocyte/pavement-cells/aggregated-cells mRNA was 1/0.00022/0.00016 for ZP1, 1/0.00103/0.00087 for ZP3 and 1/0.00019/0.00018 for ZP4 genes. In pavement-cells, ZP3 mRNA was the most expressed, followed by ZP1 and ZP4. Aggregated-cells also expressed higher levels of ZP3 mRNA, followed by ZP4 and ZP1. Pavement-cells expressed 1.19-fold more ZP3 than aggregated-cells ($p<0.05$). ZP1 and ZP4 expression was higher in pavement-cells than in aggregated-cells, yet no statistically significant difference was observed.

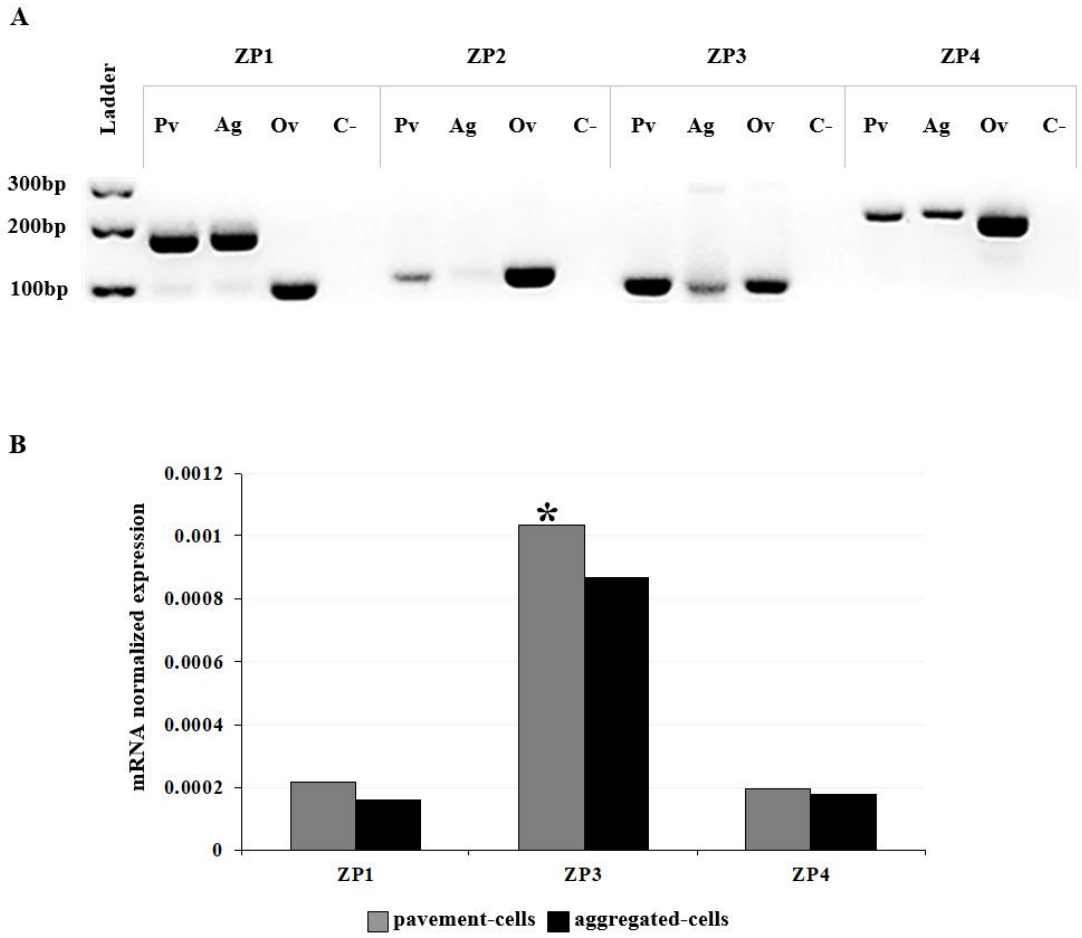

Figure 11. Molecular biology. **A**. Amplification products of ZP1, ZP2, ZP3 and ZP4 genes on PC3 pavement-cells (Pv) and aggregated-cells (Ag), oocytes (Ov) and negative control (C-). **B**. Quantification of mRNA expression by qRT-PCR. Gene expression of ZP1, ZP3 and ZP4 mRNA in PC3 pavement-cells and aggregated-cells. Normalized levels to the GAPDH reference gene and the positive control (oocyte) mRNA as reference. ZP3 mRNA expression is significantly higher in pavement-cells (*) when compared with aggregated-cells ($p<0.05$).

4. Discussion

4.1. Previous ultrastructural studies on prostate cancer tissue

In the study of Mao et al (1996), prostate carcinoma tissue cells evidenced a polymorphic morphology. The nucleus could be dense, lobulated, with margination of heterochromatin, or round and pale; the nucleolus was of the vacuolar type, or reticulated, central or peripheral. The cytoplasm could be rich or poor in free ribosomes; mitochondria could be pale with thin dense cristae, or possess a moderate dense matrix with pale cristae; RER cisternae, Golgi apparatus, dense multivesicular vesicles (bodies), secretory vesicles, secondary lysosomes and lipid droplets could also be observed. Cells exhibited short microvilli and occasional cilia, and appeared attached by tight junctions and desmosomes.

In our study, we also found two similar types of nuclear morphology. Pavement-cells presented a lobulated nucleus with a regular outline, with margination of heterochromatin, a pale matrix and a reticulated nucleolus. In aggregated-cells the nucleus was also lobulated, but

presented an irregular outline, a denser matrix, with patches of heterochromatin, and a vacuolar nucleolus. Similarly, to cancer tissue cells, we also observed RER cisternae, secondary lysosomes, rare dictiosomes and secretory vesicles (the later only in aggregated-cells), microvilli, tight junctions and desmosomes, but not abundant secretory vesicles or cilia. However, in PC3 cells, microvilli were long and mixed with stereocilia; additionally, and although we have also observed occasional multivesicular vesicles in pavement-cells, these had a pale matrix. Yet not mentioned in the text, from image analysis of the cancer tissue, we could distinguish occasional vesicles with microvilli and coated vesicles similarly to PC3-cells. The cytoplasmic organization of PC3-cells appeared quite different from cancer tissues. Pavement-cells appeared polarized: one pole showed an accumulation of dense elongated mitochondria, RER cisternae and small secondary lysosomes, and the other pole evidenced profound surface invaginations that originated a net of vesicles containing microvilli, and light mitochondria; cytochemical analysis confirmed the absence of lipid droplets and glycogen accumulation in these cells. Aggregated-cells evidenced two types of cells, one also with surface invaginations, and another rich in lipid droplets; cytochemical analysis also evidenced two types of cells, one rich in glycogen and the other rich in lipid droplets. Another difference to pavement-cells was the presence of enlarged pale cristae in dense mitochondria.

In the work of Sahlén et al (2004) of prostate cancer bone metastases, authors only described cytoplasmic organelles. Nevertheless, from one image we could observe part of a nucleus, which showed a regular outline, a pale matrix and a reticulated nucleolus. This nuclear appearance is similar to the nucleus of pavement-cells with the exception that in PC3-cells the nucleus was lobulated. In the cell surface authors observed short microvilli and prostasome exocytosis, whereas in PC3-cells we found long microvilli and stereocilia, but no signs of exocytosis. Authors did not show cell junctions, but PC3-cells evidenced tight junctions and desmosomes. In the cytoplasm of metastatic cells, images evidenced the presence of RER cisternae, Golgi complexes and numerous secretory vesicles (prostasomes); regarding the mitochondria, from the images we could also observe moderate-dense mitochondria with pale or thin dense cristae. In PC3-cells, we also observed RER cisternae, and rare dictiosomes and secretory vesicles (the later only in aggregated-cells). Regarding the mitochondria, we found different aspects, as pavement-cells showed long dense mitochondria with pale cristae and pale mitochondria with dense cristae, whereas aggregated-cells evidenced dense mitochondria with pale enlarged cristae and pale mitochondria with dense cristae.

In the study of Hetzl et al (2010), prostate cancer tissue cell images were of low resolution, which prejudiced detailed comparisons. From images we could distinguish that the nucleus was oval and of two main types, one presented a moderate-dense matrix with the nucleolus attached to the nuclear envelope, and the other presented a dense matrix with numerous heterochromatin patches. The pale nucleus resembled the nucleus of our pavement-cells, and the dense nucleus

resembled that of our aggregated-cells, with the exception that in PC3-cells the nucleus was lobulated, with a regular outline in pavement-cells and an irregular outline in aggregated-cells. The low magnification used by the authors did not allow comparisons for the type of nucleolus neither to compare the mitochondria. Nevertheless, authors described the presence of RER cisternae, Golgi apparatus, secretory vesicles and short and sparse microvilli, and do not mention the presence of secondary lysosomes, lipid droplets or cell junctions. In contrast and regarding the cell surface, in PC3-cells we found long microvilli and stereocilia, profound surface invaginations, and cell adhesion through tight junctions and desmosomes. In relation to the cytoplasm, in PC3-cells we observed RER cisternae, secondary lysosomes and lipid droplets, and rare dictiosomes and secretory vesicles (the later only in aggregated-cells).

4.2. Previous ultrastructural studies on the prostate cancer PC3 cell-line

In the study of Kaighn et al (1979), authors established and characterized the PC3 cell-line, which was derived from prostate adenocarcinoma tissues and bone metastases. Regarding cell ultrastructure, the authors divided the observations into adherent cells (that correspond to our pavement-cells) and grape-like aggregates of loosely attached cells formed above adherent cells (that correspond to our aggregated cells). In the text, authors stated that the cytoplasmic structure of the cells was similar.

As authors did not specify their findings, we thus conducted a detailed image review. The adherent cells described by the authors had a fusiform appearance and the surface contained numerous short microvilli and occasional long stereocilia; the nucleus presented an irregular outline with a moderate-dense matrix, without heterochromatin patches, and large reticulated nucleoli; at one pole of the cell, the cytoplasm was rich in long dense mitochondria and RER cisternae, with presence of a few secondary lysosomes; the other cytoplasmic pole of the cell was rich in dense mitochondria and secondary lysosomes; although described in the text, we could not discern in images the dictiosomes, annulate lamellae, lipid droplets and desmosomes. In comparison to our pavement-cells, the cell surface presented longer microvilli and numerous stereocilia, and we here demonstrate the presence of tight junctions and desmosomes. Contrary to authors, the nucleus of pavement-cells had a regular outline, was lobulated and presented a pale matrix, although they were similar regarding the absence of patches of heterochromatin and presence of reticulated nucleoli. In relation to one of the poles, pavement-cells similarly presented a high concentration of long dense mitochondria and RER cisternae, but additionally presented a higher concentration of secondary lysosomes. Concerning the other pole of the cell, authors did not observe the lacework of complex surface invaginations that we found in pavement-cells. Also contrary to author findings, we did not observe annulate lamellae or lipid droplets. Another difference was the presence of two types of mitochondria in pavement-cells. Similarly to authors, we observed a high number of ribosomes, which were here proved to not be glycogen particles.

The spherical cell aggregates described by the authors were oval, and showed scarce and short microvilli; the nucleus was eccentrically located, possessed an irregular outline, contained a moderate-dense matrix, without heterochromatin patches, and large reticulated nucleoli; the cytoplasm showed aggregates of dense mitochondria, large vesicles with presence of microvilli and numerous large secondary lysosomes; although not shown in the micrograph, authors described the presence of Golgi complexes, RER cisternae, annulate lamellae, lipid droplets, tight junctions and desmosomes. In comparison to our aggregated-cells, the cell surface presented long microvilli and stereocilia, and we here demonstrate the presence of tight junctions and desmosomes. In contrast, the nucleus of our aggregated-cells was profoundly irregular, lobulated and presented a denser matrix, filled with patches of heterochromatin, and vacuolar nucleoli. Moreover, we observed two main types of cells, one filled with light vesicles presenting microvilli formed subsequently to a profound invagination of the cell surface at one pole of the cell, and another filled with lipid droplets. Also oppositely, we did not observe annulate lamellae, but we have similarly found numerous RER cisternae. Another difference was the presence of two types of mitochondria in aggregated-cells. Similarly to authors, we observed a high number of small cytoplasmic granules, which were here proved to be glycogen particles.

In the work of Ravenna et al (1996), authors studied the effect of the n-Hexane lipid/sterol plant extract on PC3-cells. There is only one ultrastructural image of a normal cell. In the image, a round cell at metaphase is superposed on two elongated cells. The connections between those cells could not be identified due to the low image magnification. Elongated cells had an irregular nucleus without heterochromatin patches and several nucleoli, but details are not possible to infer due to the low magnification of the image. Although not visible due to the low magnification, authors described the existence of numerous mitochondria and a scarce presence of other organelles. We thus had no data for comparisons with our pavement-cells. Regarding the round cell, which probably corresponds to our aggregated-cells, it is in metaphase and thus comparisons could not be performed.

In the study of Kim et al (2005), authors analysed the effect of the plant extracted andrographolide on PC3-cells. There is only one ultrastructural image of a normal cell. This cell is ovoid and the nucleus has a moderate-dense matrix, with patches of internal and peripheral heterochromatin and a large peripheral nucleolus. This resembles the nucleus of our aggregated-cells. In the image, aggregated dense mitochondria and large vesicles could be observed, but the low magnification did not allow further comparisons with our observations.

In the work of You et al (2015), authors studied the effect of sodium metaarsenite on PC3-cells. There is only one ultrastructural image of a normal cell. This cell was oval and the nucleus had a moderate-dense matrix, without patches of heterochromatin, and a central nucleolus. This resembles the nucleus of our aggregated-cells except that these have patches of heterochromatin, and the nucleolus is peripheral. Other nuclear and cytoplasmic features could not be compared

with our observations due to the low magnification used. The cell appears to present microvilli and do not exhibit evident connections to adjacent cells. On the contrary, our aggregated-cells possess prominent microvilli and stereocilia, and evident connections.

In the study of Xu et al (2016), authors studied the effect of dihydroartemisinin on PC3-cells. There is only one ultrastructural image of a normal cell. This cell was oval and the nucleus had a moderate-dense matrix with patches of internal and peripheral heterochromatin. This resembles the nucleus of our aggregated-cells. In the image, mitochondria, RER cisternae and small vesicles could be observed, but the low magnification did not allow for comparisons with our observations.

4.3. Previous studies on cancers expressing ZP3

In the work of Rahman et al (2012), authors found expression of ZP3 in the cytoplasm of human granulosa cell-lines, granulosa tumors and surface ovarian cancer. There are no ultrastructural images. Using recombinant ZP3, authors were able to treat ovarian cancer through immunization against ZP3.

In the report of Bennink (2016), the author submitted a patent on prostate cancer, where the author developed a method to improve the immune response against these cancer cells. The author evidenced ZP3 expression in prostate tumor cells and observed that an immune killer response against prostate cancer cells could be induced using ZP3 as antigen. Additionally, the author showed expression of ZP3 in the cytoplasm of human prostate adenocarcinoma tissue cells and in PC3-cells, but not in normal prostate tissue. All these images are in black-white and there are no ultrastructural images. These findings were confirmed by immunocytochemistry and mRNA expression. Regarding our immunohistochemical observations we not only also found ZP3 staining in the cytoplasm of prostate adenocarcinoma tissue cells, but staining was also observed at the cell surface; additionally, we also observed cytoplasmic and surface staining for the other ZP glycoproteins, ZP1, ZP2 and ZP4 in prostate cancer tissue. We further evaluated PC3-cells by immunocytochemistry and mRNA expression, not on total cells as authors did, but on separate pavement-cells and aggregated-cells. We observed surface and cytoplasmic expression in both cell types regarding the four ZP glycoproteins, and confirmed mRNA expression by quantitative PCR.

4.4. Molecular biology

In the present study, we demonstrated that the mRNA of ZP1, ZP3 and ZP4 genes is expressed in PC3-cells. PCR products from each gene were confirmed by Sanger sequencing, which proved the specificity of PCR products. Further, ZP1, ZP3 and ZP4 mRNA expression, as demonstrated by RT-PCR, was in accordance with immunofluorescence results. However, the PCR product of ZP1 exhibited a higher size than what was expected. Product specificity was confirmed by Sanger sequencing, and the higher size was shown to be due to intron retention. Given that genomic DNA

was digested prior to amplification and all the other genes (amplified using the same cDNA) had the expected sequence, it is unlikely that this could be due to a genomic DNA contamination. Therefore, we hypothesize that the PC3 cell-line expresses a variant of the ZP1 mRNA, which holds an intron sequence. At the Ensembl database (Ensembl Release 93; July 2018) three other transcripts with intron retention are described. These corresponded to major events leading to loss of four, eight or nine exons, respectively, which gave rise to a nonfunctional protein. On the contrary, we here present a case of intron retention in ZP1 in the prostate cancer PC3 cell-line that apparently did not affect protein production as it was present in immunocytochemical experiences. Intron retention has been associated with cancer molecular phenotype. This phenomenon can result in an inactivated protein and, when it happens at a tumor suppressor protein, it gives advantage to tumor cells (Jung et al., 2015). Also, intron-retaining mRNAs are known to play essential roles in normal physiology and disease, and in prostate cancer it has been related to microRNA expression regulation (Wong et al., 2016).

ZP2 amplification resulted in an inconspicuous PCR product in pavement-cells that, after sequencing, showed no significant similarity with any transcript. Several PCR conditions were tested and still the existing techniques applied within this study were not sensitive enough to detect it. These results could indicate that the mRNA expression of ZP2 is very low, or even absent, in PC3-cells. Notwithstanding, ZP2 protein expression was positive on immunofluorescence assays, which seems to contradict the gene expression results. However, mRNA and protein levels correlations are not as linear. In fact, it is generally reported a poor correlation between the levels of mRNA and protein expression (Greenbaum et al., 2003). Biologically, this poor correlation could be explained by post-transcriptional and post-translational modifications, as well as by the possibility that proteins have very different half-lives (Greenbaum et al., 2003). In this case, a low mRNA stability or a rapid mRNA turnover could justify the presence of the ZP2 protein without concomitant mRNA expression (Vogel and Marcotte, 2012).

Data from HPA have no records on protein expression of ZP1 in prostate normal and cancer tissue, or prostate cancer cell-lines. We observed protein expression in cancer tissue and PC3-cells. This difference can be justified by the fact that HPA data is based on genome-wide analysis of human proteins that, although very useful and breakthrough, can be problematic because the massive number of data has a great potential for false-positive/negative results (Pearson and Manolio, 2008). Relatively to RNA expression, the HPA database found expression in prostate cancer, but not in normal prostate tissue or prostate cancer cell-lines. We not only found mRNA expression in prostate cancer, but also in PC3-cells. Regarding ZP2, data from HPA showed that the prostate cancer tissue express the ZP2 glycoprotein, but not mRNA. We here confirm ZP2 protein expression in prostate cancer tissue and in PC3-cells, and that mRNA expression in PC3-cells was not detected. In relation to ZP3, data from HPA showed no protein expression of ZP3

in prostate normal or cancer tissues. In relation to mRNA expression, HPA data revealed RNA expression of ZP3 in prostate normal and cancer tissue, and in PC3-cells. Protein and mRNA expression of ZP3 was found in prostate cancer tissue and PC3-cells, but not in normal prostate tissue (Bennink, 2016), which is in accordance to our present results. Additionally, we also discriminated ZP3 expression according to the growth pattern of this cell-line. We demonstrated that pavement-cells express 1.19-fold more ZP3 mRNA than aggregated-cells ($p<0.05$). The human ZP, among all its functions, is responsible for preventing immune rejection of the pre-implantation embryo. Assuming that cancer cells, in order to evolve, make use of all cell potential, it will not be so strange to think that cancer cells can express ZP proteins to evade immune rejection. Being true, pavement-cells, which have a similar morphology with the invading cells, have a higher necessity to evade immune rejection and for that reason need to express a higher level of ZP proteins. On the other hand, aggregated-cells are more similar to the in-situ tumor and may not have such need for immune evasion. Nevertheless, further studies are needed to unveil the existence of pathophysiological consequences of this ZP3 mRNA expression differences in pavement-cells and aggregated-cells. Data from HPA have no records on protein or mRNA expression of ZP4 in prostate normal and cancer tissue, or prostate cancer cell-lines. On the contrary, we here give evidence for protein and mRNA expression of ZP4 in both prostate adenocarcinoma tissue and PC3-cells.

5. Conclusion

We found substantial differences on the ultrastructure of PC3-cells. We believe that this was due to the detailed analysis here performed. We here firstly describe that pavement-cells are polarized, with one of the poles exhibiting profound surface invaginations, whose fate and function remain to be explored; another difference relates to the presence of two types of mitochondria in opposite poles of pavement-cells. Two types of aggregated-cells were observed, one exhibiting surface invaginations, and the other being rich in lipid droplets; the morphology of mitochondria found in both cell-types was also different, and aggregated-cells with surface invaginations were rich in glycogen. We here also firstly show the detection of the four oocyte ZP glycoproteins in the cell surface and cytoplasm of prostate adenocarcinoma tissue cells and PC3-cells. These observations were further expanded by the detection of mRNA expression of ZP1, ZP3 and ZP4 in both pavement-cells and aggregated-cells, but not of ZP2. Additionally, we showed that the mRNA transcript of ZP1 presents intron retention, but for the moment, we do not know if this affects protein structure and function.

6. References

Bennink, H.J.T.C., inventor, 2016. Pantarhei Bioscience BV, Zeist, Netherlands, assignee. Immunotherapeutic method for treating prostate cancer. US patent 9,295,720 B2. Mar. 2016. https://patents.google.com/patent/US9295720

Eisenberg, E., Levanon, E.Y., 2013. Human housekeeping genes, revisited. Trends. Genet. 29(10), 569-574. https://doi.org/10.1016/j.tig.2013.05.010

Greenbaum, D., Colangelo, C., Williams, K., Gerstein, M., 2003. Comparing protein abundance and mRNA expression levels on a genomic scale. Genome Biol. 4(9), 117. https://doi.org/10.1186/gb-2003-4-9-117

Gupta, S.K., Jethanandani, P., Afzalpurkar, A., Kaul, R., Santhanam, R., 1997. Prospects of zona pellucida glycoproteins as immunogens for contraceptive vaccine. Hum. Reprod. Update. 3(4), 311-324. https://doi.org/10.1093/humupd/3.4.311

Gupta, S.K., Bhandari, B., Shrestha, A., Biswal, B.K., Palaniappan, C., Malhotra, S.S., Gupta, N., 2012. Mammalian zona pellucida glycoproteins: structure and function during fertilization. Cell Tiss. Res. 349(3), 665-678. https://doi.org/10.1007/s00441-011-1319-y

Hasegawa, A., Tanaka, H., Shibahara, H., 2014. Infertility and immunocontraception based on zona pellucida. Reprod. Med. Biol. 13(1), 1-9. https://doi.org/10.1007/s12522-013-0159-8

Hetzl, A.C., Favaro, W.J., Billis, A., Ferreira, U., Cagnon, V.H.A., 2010. Prostatic diseases in the senescence: structural and proliferative features. Aging Male. 13(2), 124-132. https://doi.org/10.3109/13685531003586991

Jung, H., Lee, D., Lee, J., Park, D., Kim, Y.J., Park, W.Y., Hong, D., Park, P.J., Lee, E., 2015. Intron retention is a widespread mechanism of tumor-suppressor inactivation. Nat. Genet. 47(11), 1242-1248. https://doi.org/10.1038/ng.3414

Kaighn, M.E., Narayan, S., Ohnuki, Y., Lechner, J.F., Jones, L.W., 1979. Establishment and characterization of a human prostatic carcinoma cell line (PC-3). Invest. Urol. 17(1), 16-23. https://www.ncbi.nlm.nih.gov/pubmed/447482

Kim, T.G., Hwi, K.K., Hung, C.S., 2005. Morphological and biochemical changes of andrographolide-induced cell death in human prostatic adenocarcinoma PC-3 cells. In vivo (Athens, Greece). 19(3), 551-558. https://www.ncbi.nlm.nih.gov/pubmed/15875775

Lefièvre, L., Conner, S.J., Salpekar, A., Olufowobi, O., Ashton, P., Pavlovic, B., Lenton, W., Afnan, M., Brewis, I.A., Monk, M., Hughes, D.C., Barratt, C.L.R., 2004. Four zona pellucida glycoproteins are expressed in the human. Hum. Reprod. 19(7), 1580-1586. https://doi.org/10.1093/humrep/deh301

Mao, P., Nakao, K., Angrist, A., 1966. Human prostatic carcinoma: an electron microscope study. Cancer Res. 26(5), 955-973. https://www.ncbi.nlm.nih.gov/pubmed/5934805

Morgulis, A., Coulouris, G., Raytselis, Y., Madden, T.L., Agarwala, R., Schäffer, A.A., 2008. Database Indexing for Production MegaBLAST Searches. Bioinformatics 24(16), 1757-1764. https://doi.org/10.1093/bioinformatics/btn322

Pfaffl, M.W., 2001. A new mathematical model for relative quantification in real-time RT-PCR. Nucleic Acids Res. 29(9), e45. https://doi.org/10.1093/nar/29.9.e45

Pearson, T.A., Manolio, T.A., 2008. How to Interpret a Genome-wide Association Study. JAMA 299(1), 1335-1344. https://doi.org/10.1001/jama.299.11.1335

Rahman, N.A., Bennink, H.J.T.C., Chrusciel, M., Dharp, V., Zimmerman, Y., Dina, R., Li, X., Ellone, A., Rivero-Muller, A., Dilworth, S., Ghaem-Maghami, S., Vainio, O., Huhtaniemi, I., 2012. A novel treatment strategy for ovarian cancer based on immunization against zona pellucida protein (ZP) 3. FASEB J. 26(1), 324-333. https://doi.org/10.1096/fj.11-192468

Ravenna, L., Di Silverio, F., Russo, M.A., Salvatori, L., Morgante, E., Morrone, S., Cardillo, M.R., Russo, A., Frati, L., Gulino, A., Petrangeli, E., 1996. Effects of the lipidosterolic extract of Serenoa repens (Permixon) on human prostatic cell lines. Prostate. 29(4), 219-230. https://doi.org/10.1002/(SICI)1097-0045(199610)29:4<219::AID-PROS3>3.0.CO;2-6

Sá, R., Cunha, M., Silva, J., Luís, A., Oliveira, C., Teixeira da Silva, J., Barros, A., Sousa, M., 2011. Ultrastructure of tubular smooth endoplasmic reticulum aggregates in human metaphase II oocytes and clinical implications. Fertil. Steril. 96(1), 143-149.e7. https://doi.org/10.1016/j.fertnstert.2011.04.088

Sahlén, G., Ahlander, A., Frost, A., Ronquist, G., Norlén, B.J., Nilsson, B.O., 2004. Prostasomes are secreted from poorly differentiated cells of prostate cancer metastases. Prostate. 61(3), 291-297. https://doi.org/10.1002/pros.20090

Sousa, M., Teixeira da Silva, J., Silva, J., Cunha, M., Viana, P., Oliveira, E., Sá, R., Soares, C., Oliveira, C., Barros, A., 2015. Embryological, clinical and ultrastructural study of human oocytes presenting indented zona pellucida. Zygote. 23(1), 145-157. https://doi.org/10.1017/S0967199413000403

Tai, S., Sun, Y., Squires, J.M., Zhang, H., Oh, W.K., Liang, C.-Z., Huang, J., 2011. PC3 is a Cell line characteristic of prostatic small cell carcinoma. Prostate. 71(15), 1668-1679. https://doi.org/10.1002/pros.21383

The human protein atlas. Version 18, 14th of June of 2018. Available from www.proteinatlas.org

van Bokhoven, A., Varella-Garcia, M., Korch, C., Johannes, W.U., Smith, E.E., Miller, H.L., Nordeen, S.K., Miller, G.J., Lucia, M.S., 2003. Molecular characterization of human prostate carcinoma cell lines. Prostate. 57(3), 205-225. https://doi.org/10.1002/pros.10290

Vogel, C., Marcotte, E.M., 2012. Insights into the regulation of protein abundance from proteomic and transcriptomic analyses. Nat. Rev. Genet. 13(4), 227-232. https://doi.org/10.1038/nrg3185

Wassarman, P.M., 2008. Zona pellucida glycoproteins. J. Biol. Chem. 283(36), 24285-27289. https://doi.org/10.1074/jbc.R800027200

Wong, J.J.-L., Au, A.Y.M., Ritchie, W., Rasko, J.E.J., 2016. Intron retention in mRNA: no longer nonsense. Bioessays. 38(1), 41-49. https://doi.org/10.1002/bies.201500117

Xu, G., Zou, W.-Q., Du, S.-J., Wu, M.-J., Xiang, T.-X., Luo, Z.-G., 2016. Mechanism of dihydroartemisinin-induced apoptosis in prostate cancer PC3 cells: An iTRAQ-based proteomic analysis. Life Sci. 157:1-11. https://doi.org/10.1016/j.lfs.2016.05.033

Ye, J., Coulouris, G., Zaretskaya, I., Cutcutache, I., Rozen, S., Madden, T.L., 2012. Primer-BLAST: a tool to design target-specific primers for polymerase chain reaction. BMC Bioinformatics 13, 134. https://doi.org/10.1186/1471-2105-13-134

You, D., Kim, Y., Jang, M.J., Lee, C., Jeong, I.G., Cho, Y.M., Hwang, J.J., Hong, J.H., Ahn, H., Kim, C.-S., 2015. KML001 induces apoptosis and autophagic cell death in prostate cancer cells via oxidative stress pathway. PLOS ONE. 10(9), e0137589. https://doi.org/10.1371/journal.pone.0137589

Zhang, Z., Schwartz, S., Wagner, L., Miller, W., 2000. A greedy algorithm for aligning DNA sequences. J. Comput. Biol. 7, 203-214. https://doi.org/10.1089/10665270050081478

IV. FINAL REMARKS

Prostate cancer is a highly incident type of cancer which has seen its molecular biology scrutinized. However, little attention has been given to its morphology especially that of the cell-lines routinely used on current investigation. PC3 is one of the cell-lines used since long ago, yet its ultrastructural morphology is not fully understood. In this work we performed a detailed description of the cells from this cell-line.

First, two types of growth were identified, adherent growth (pavement-cells) and growth in suspension (aggregated-cells). The two types of cells, pavement and aggregated, showed distinct ultrastructural characteristics. Pavement-cells present a polarized architecture with two types of mitochondria in opposite poles. Aggregated-cells were constituted by two different cell-types, one rich in glycogen and exhibiting surface invaginations and the other being rich in lipid droplets.

Second, the expression of ZP1-ZP4 proteins was found in both prostate cancer tissue and pavement and aggregated PC3-cells but not in normal prostate tissue. ZP1, ZP3 and ZP4 gene expression was found in both pavement and aggregated cells, with pavement-cells presenting higher expression levels of all proteins. ZP3 was the most expressed gene in both pavement and aggregated cells. Additionally, we showed that the ZP1 mRNA transcript was a variant with intron retention, a phenomenon that has been associated with cancer cells.

As development of immune-based therapies against ZP proteins for the treatment of prostate cancer are being developed, our present results can thus strongly contribute to this oncology field. Nevertheless, further studies are required to identify the mechanisms behind the expression of the four oocyte ZP glycoproteins in prostate cancer tissue and cell-lines.

V. FUTURE PERSPETIVES

Zona pellucida and prostate cancer: the intriguing connection

The present work firstly describes the detailed ultrastructure of the cells from the PC3 cell-line. However, other cell-lines from the prostate carcinoma are routinely used, namely LNCaP and DU145, which lack a detailed description of their ultrastructure. Their description will be of great interest not only to better understand the nature of those cells but also to compare them with the ultrastructural characteristics of PC3-cells and identify the differences between them.

Protein expression of ZP1-ZP4 was evaluated on both prostate cancer tissue and PC3-cells, being firstly found the expression of all proteins in both tissue and cells. It will be interesting to evaluate if other cell-lines from prostate carcinoma also express ZP1-ZP4 proteins and to assess the expression of the ZP1-ZP4 genes.

The expression of the ZP proteins in prostate cancer tissue and cells does not have a plausible justification and further studies are required to uncover the mechanisms that lead to the expression of ZP1-ZP4 proteins in the tumoral tissue since normal tissue does not express ZP proteins. Since PC3-cells expressed ZP proteins, a possible assay would be to silence the expression of ZP proteins and evaluate the effects of gene silencing by proliferation, migration and invasion assays.

One of the main participants in this story is the ZP-domain, which has been described to be present in several proteins associated with cancer, but its exact function remains to be unveiled. We believe that the discovery of the functions of the ZP-domain will be a huge step towards understanding of these proteins and their association with cancer.

VI. REFERENCES

Balza E, Castellani P, Zijlstra A, Neri D, Zardi L, Siri A. Lack of specificity of endoglin expression for tumor blood vessels. Int J Cancer. 2001;94(4):579-585. https://doi.org/10.1002/ijc.1505

Bennink, H.J.T.C., inventor, 2016. Pantarhei Bioscience BV, Zeist, Netherlands, assignee. Immunotherapeutic method for treating prostate cancer. US patent 9,295,720 B2. Mar. 2016. https://patents.google.com/patent/US9295720

Burrows FJ, Derbyshire EJ, Tazzari PL, Amlot P, Gazdar AF, King SW, Letarte M, Vitetta ES, Thorpe PE. Up-regulation of endoglin on vascular endothelial cells in human solid tumors: implications for diagnosis and therapy. Clin Cancer Res. 1995;1(12):1623-1634. https://www.ncbi.nlm.nih.gov/pubmed/9815965

Calabrò L, Fonsatti E, Bellomo G, Alonci A, Colizzi F, Sigalotti L, Altomonte M, Musolino C, Maio M. Differential levels of soluble endoglin (CD105) in myeloid malignancies. J Cell Physiol. 2003;194(2):171-175. https://doi.org/10.1002/jcp.10200

Chen T, Bian Y, Liu X, Zhao S, Wu K, Yan L, Li M, Yang Z, Liu H, Zhao H, Chen ZJ. A Recurrent Missense Mutation in ZP3 Causes Empty Follicle Syndrome and Female Infertility. Am J Hum Genet. 2017;101(3):459-465. https://doi.org/10.1016/j.ajhg.2017.08.001

Clark GF, Oehninger S, Patankar MS, Koistinen R, Dell A, Morris HR, Koistinen H, Seppälä M. A role for glycoconjugates in human development: the human feto-embryonic defence system hypothesis. Hum Reprod. 1996;11(3):467-473. https://doi.org/10.1093/HUMREP/11.3.467

Colombatti A, Bonaldo P, Doliana R. Type A modules: interacting domains found in several non-fibrillar collagens and in other extracellular matrix proteins. Matrix. 1993;13(4):297-306. https://doi.org/10.1016/S0934-8832(11)80025-9

Curtis P, Burford G, Amso N, Keith E, Shaw RW. Assessment of the relevance of zona pellucida antibodies in serum and cervical mucus in patients who have fertilization failure during in vitro fertilization. Fertil Steril. 1991;56(6):1124-1127. https://doi.org/10.1016/S0015-0282(16)54727-X

Ewoldsen MA, Ostlie NS, Warner CM. Killing of mouse blastocyst stage embryos by cytotoxic T lymphocytes directed to major histocompatibility complex antigens. J Immunol. 1987;138(9):2764-2770. https://www.ncbi.nlm.nih.gov/pubmed/3494769

Fant M, Farina A, Nagaraja R, Schlessinger D. PLAC1 (Placenta-specific 1): a novel, X-linked gene with roles in reproductive and cancer biology. Prenat Diagn. 2010;30(6):497-502. https://doi.org/10.1002/pd.2506

Fonsatti E, Altomonte M, Nicotra MR, Natali PG, Maio M. Endoglin (CD105): a powerful therapeutic target on tumor-associated angiogenetic blood vessels. Oncogene. 2003;22(42):6557-6563. https://doi.org/10.1038/sj.onc.1206813

Fonsatti E, Del Vecchio L, Altomonte M, Sigalotti L, Nicotra MR, Coral S, Natali PG, Maio M. Endoglin: An accessory component of the TGF-beta-binding receptor complex with diagnostic, prognostic, and bioimmunotherapeutic potential in human malignancies. J Cell Physiol. 2001;188(1):1-7. https://doi.org/10.1002/jcp.1095

Ghods R, Ghahremani MH, Madjd Z, Asgari M, Abolhasani M, Tavasoli S, Mahmoudi AR, Darzi M, Pasalar P, Jeddi-Tehrani M, Zarnani AH. High placenta-specific 1/low prostate-specific antigen expression pattern in high-grade prostate adenocarcinoma. Cancer Immunol Immunother. 2014;63(12):1319-1327. https://doi.org/10.1007/s00262-014-1594-z

Gook D, Edgar D, Borg J, Martic M. Detection of zona pellucida proteins during human folliculogenesis. Hum Reprod. 2008;23(2):394-402. https://doi.org/10.1093/humrep/dem373

Goudet G, Mugnier S, Callebaut I, Monget P. Phylogenetic analysis and identification of pseudogenes reveal a progressive loss of zona pellucida genes during evolution of vertebrades. Biol Reprod. 2008;78(5):796-806. https://doi.org/10.1095/biolreprod.107.064568

Grasa P, Kaune H, Williams SA. Embryos generated from oocytes lacking complex N- and O-glycans have compromised development and implantation. Reproduction. 2012;144(4):455-465. https://doi.org/10.1530/REP-12-0084

Green DP. Three-dimensional structure of the zona pellucida. Rev Reprod. 1997;2(3):147-156. https://doi.org/10.1530/revreprod/2.3.147

Gupta SK, Bhandari B, Shrestha A, Biswal BK, Palaniappan C, Malhotra SS, Gupta N. Mammalian zona pellucida glycoproteins: structure and function during fertilization. Cell Tissue Res. 2012;349(3):665-678. https://doi.org/10.1007/s00441-011-1319-y

Hovav Y, Almagor M, Benbenishti D, Margalioth EJ, Kafka I, Yaffe H. Immunity to zona pellucida in women with low response to ovarian stimulation, in unexplained infertility and after multiple IVF attempts. Hum Reprod. 1994;9(4):643-645. https://doi.org/10.1093/oxfordjournals.humrep.a138563

Huang H-L, Lv C, Zhao Y-C, Li W, He X-M, Li P, Sha AG, Tian X, Papasian CJ, Deng HW, Lu GX, Xiao HM. Mutant ZP1 in familial infertility. N Engl J Med. 2014;370(13):1220-1226. https://doi.org/10.1056/NEJMoa1308851

Hughes D, Barratt CLR. Identification of the true human orthologue of the mouse ZP1 gene: evidence for greater complexity in the mammalian zona pellucida? Biochim Biophys Acta. 1999;1447(2-3):303-306. https://doi.org/10.1016/s0167-4781(99)00181-5

Huo Y, Xu Y, Wang J, Wang F, Liu Y, Zhang Y, Zhang B. Analysis of the serum reproductive system related autoantibodies of infertility patients in Tianjin region of China. Int J Clin Exp Med. 2015;8(8):14048-14053. https://www.ncbi.nlm.nih.gov/pubmed/26550366

Jimenez-Movilla M, Dean J. ZP2 and ZP3 cytoplasmic tails prevent premature interactions and ensure incorporation into the zona pellucida. J Cell Sci. 2011;124(Pt 6):940-950. https://doi.org/10.1242/jcs.079988

Kamada M, Hasebe H, Irahara M, Kinoshita T, Naka O, Mori T. Detection of anti-zona pellucida activities in human sera by the passive hemagglutination reaction. Fertil Steril. 1984;41(6):901-906. https://doi.org/10.1016/S0015-0282(16)47905-7

Kelkar RL, Meherji PK, Kadam SS, Gupta SK, Nandedkar TD. Circulating auto-antibodies against the zona pellucida and thyroid microsomal antigen in women with premature ovarian failure. J Reprod Immunol. 2005;66(1):53-67. https://doi.org/10.1016/j.jri.2005.02.003

Lefièvre L, Conner SJ, Salpekar A, Olufowobi O, Ashton P, Pavlovic B, Lenton W, Afnan M, Brewis IA, Monk M, Hughes DC, Barratt CL. Four zona pellucida glycoproteins are expressed in the human. Hum Reprod. 2004;19(7):1580-1586. https://doi.org/10.1093/humrep/deh301

Leong CT, Ong CK, Tay SK, Huynh H. Silencing expression of UO-44 (CUZD1) using small interfering RNA sensitizes human ovarian cancer cells to cisplatin in vitro. Oncogene. 2007;26(6):870-880. https://doi.org/10.1038/sj.onc.1209836

Leong CTC, Ng CY, Ong CK, Ng CP, Ma ZS, Nguyen TH, Tay SK, Huynh H. Molecular cloning, characterization and isolation of novel spliced variants of the human ortholog of a rat estrogen-regulated membrane-associated protein, UO-44. Oncogene. 2004;23(33):5707-5718. https://doi.org/10.1038/sj.onc.1207754

Leube B, Drechsler M, Mühlmann K, Schäfer R, Schulz WA, Santourlidis S, Anastasiadis A, Ackermann R, Visakorpi T, Müller W, Royer-Pokora B. Refined mapping of allele loss at chromosome 10q23-26 in prostate cancer. Prostate. 2002;50(3):135-144. https://doi.org/10.1002/pros.10038

Leung F, Soosaipillai A, Kulasingam V, Diamandis EP. CUB and zona pellucida-like domain-containing protein 1 (CUZD1): a novel serological biomarker for ovarian cancer. Clin Biochem. 2012;45(18):1543-1546. https://doi.org/10.1016/j.clinbiochem.2012.08.011

Li C, Hampson IN, Hampson L, Kumar P, Bernabeu C, Kumar S. CD105 antagonizes the inhibitory signaling of transforming growth factor beta1 on human vascular endothelial cells. FASEB J. 2000;14(1):55-64. https://doi.org/10.1096/fasebj.14.1.55

Li Q, Liu M, Wu M, Zhou X, Wang S, Hu Y, Wang Y, He Y, Zeng X, Chen J, Liu Q, Xiao D, Hu X, Liu W. PLAC1-specific TCR-engineered T cells mediate antigen-specific antitumor effects in breast cancer. Oncol Lett. 2018;15(4):5924-5932. https://doi.org/10.3892/ol.2018.8075

Liaskos C, Rigopoulou EI, Orfanidou T, Bogdanos DP, Papandreou CN. CUZD1 and anti-CUZD1 antibodies as markers of cancer and inflammatory bowel diseases. Clin Dev Immunol. 2013;2013:968041. https://doi.org/10.1155/2013/968041

Liso A, Massenzio F, Stracci F. PLAC1 immunization does not induce infertility in mice. Immunotherapy. 2017;9(6):481-486. https://doi.org/10.2217/imt-2017-0019

Litcher ES, Wassarman PM. Mammalian zona pellucida domain proteins. In: Uversky VN, editor. A guide to zona pellucida domain proteins. John Wiley & Sons; 2015. p.53-86. https://doi.org/10.1002/9781119044765

Liu W, Li K, Bai D, Yin J, Tang Y, Chi F, Zhang L, Wang Y, Pan J, Liang S, Guo Y, Ruan J, Kou X, et al. Dosage effects of ZP2 and ZP3 heterozygous mutations cause human infertility. Hum Genet. 2017;136(8):975-985. https://doi.org/10.1007/s00439-017-1822-7

Liu Y, Jovanovic B, Pins M, Lee C, Bergan RC. Over expression of endoglin in human prostate cancer suppresses cell detachment, migration and invasion. Oncogene. 2002;21(54):8272-8281. https://doi.org/10.1038/sj.onc.1206117

Makabe S, Naguro T, Stallone T. Oocyte-follicle cell interactions during ovarian follicle development, as seen by high resolution scanning and transmission electron microscopy in humans. Microsc Res Tech. 2006;69(6):436-449. https://doi.org/10.1002/jemt.20303

Mannikko M, Tormala RM, Tuuri T, Haltia A, Martikainen H, Ala-Kokko L, Tapanainen JS, Lakkakorpi JT. Association between sequence variations in genes encoding human zona pellucida glycoproteins and fertilization failure in IVF. Hum Reprod. 2005;20(6):1578-1585. https://doi.org/10.1093/humrep/deh837

Mapes J, Anandan L, Li Q, Neff A, Clevenger CV, Bagchi IC, Bagchi MK. Aberrantly high expression of the CUB and zona pellucida-like domain-containing protein 1 (CUZD1) in mammary epithelium leads to breast tumorigenesis. J Biol Chem. 2018;293(8):2850-2864. https://doi.org/10.1074/jbc.RA117.000162

Meczekalski B, Nawrot R, Nowak W, Czyzyk A, Kedzia H, Gozdzicka-Jozefiak A. Study on the zona pellucida 4 (ZP4) gene sequence and its expression in the ovaries of patients with polycystic ovary syndrome. J Endocrinol Invest. 2015;38(7):791-797. https://doi.org/10.1007/s40618-015-0260-4

Nassiri F, Cusimano MD, Scheithauer BW, Rotondo F, Fazio A, Yousef GM, Syro LV, Kovacs K, Lloyd RV. Endoglin (CD105): a review of its role in angiogenesis and tumor diagnosis, progression and therapy. Anticancer Res. 2011;31(6):2283-2290. https://www.ncbi.nlm.nih.gov/pubmed/21737653

Pelletier C, Keefe DL, Trimarchi JR. Noninvasive polarized light microscopy quantitatively distinguishes the multilaminar structure of the zona pellucida of living human eggs and embryos. Fertil Steril. 2004;81(suppl 1):850-856. https://doi.org/10.1016/j.fertnstert.2003.09.033

Plaza S, Chanut-Delalande H, Fernandes I, Wassarman PM, Payre F. From A to Z: apical structures and zona pellucida-domain proteins. Trends Cell Biol. 2010;20(9):524-532. https://doi.org/10.1016/j.tcb.2010.06.002

Pokkyla RM, Lakkakorpi JT, Nuojua-Huttunen SH, Tapanainen JS. Sequence variations in human ZP genes as potential modifiers of zona pellucida architecture. Fertil Steril. 2011;95(8):2669-2672. https://doi.org/10.1016/j.fertnstert.2011.01.168

Prassas I, Brinc D, Farkona S, Leung F, Dimitromanolakis A, Chrystoja CC, Brand R, Kulasingam V, Blasutig IM, Diamandis EP. False biomarker discovery due to reactivity of a commercial ELISA for CUZD1 with cancer antigen CA125. Clin Chem. 2014;60(2):381-388. https://doi.org/10.1373/clinchem.2013.215236

Rahman NA, Bennink HJ, Chrusciel M, Sharp V, Zimmerman Y, Dina R, Li X, Ellonen A, Rivero-Müller A, Dilworth S, Ghaem-Maghami S, Vainio O, Huhtaniemi I. A novel treatment strategy for ovarian cancer based on immunization against zona pellucida protein (ZP) 3. FASEB J. 2012;26(1):324-333. https://doi.org/10.1096/fj.11-192468

Rosen LS, Gordon MS, Robert F, Matei DE. Endoglin for targeted cancer treatment. Curr Oncol Rep. 2014;16(2):365. https://doi.org/10.1007/s11912-013-0365-x

Sá R, Barros A, Sousa M. Acrosomic reaction and fertilization. In: Fardilha M, Vieira Silva J, Conde M, editors. Male human reproduction: fundamental principles. ARC Publishing; 2015. p.123-130. https://www.arc-publishing.org/Human-male-reproduction.html

Sá R, Cunha M, Silva J, Luís A, Oliveira C, Teixeira Da Silva J, Barros A, Sousa M. Ultrastructure of tubular smooth endoplasmic reticulum aggregates in human metaphase II oocytes and clinical implications. Fertil Steril. 2011;96(1):143-149. https://doi.org/10.1016/j.fertnstert.2011.04.088

Sacco AG, Moghissi KS. Anti-zona pellucida activity in human sera. Fertil Steril. 1979;31(5):503-506. https://doi.org/10.1016/S0015-0282(16)43993-2

Seon BK. Expression of endoglin (CD105) in tumor blood vessels. Int J Cancer. 2002;99(2):310-311. https://doi.org/10.1002/ijc.10378

Seshagiri PB, Vani V, Madhulika P. Cytokines and blastocyst hatching. Am J Reprod Immunol. 2016;75(3):208-217. https://doi.org/10.1111/aji.12464

Shivers CA, Dunbar BS. Autoantibodies to zona pellucida: a possible cause for infertility in women. Science. 1977;197(4308):1082-1084. https://doi.org/10.1126/science.70076

Somerville RP, Shoshan Y, Eng C, Barnett G, Miller D, Cowell JK. Molecular analysis of two putative tumour suppressor genes, PTEN and DMBT, which have been implicated in glioblastoma multiforme disease progression. Oncogene. 1998;17(13):1755-1757. https://doi.org/10.1038/sj.onc.1202066

Sousa M, Cunha M, Silva J, Oliveira E, Pinho MJ, Almeida C, Sá R, Teixeira da Silva J, Oliveira C, Barros A. Ultrastructural and cytogenetic analyses of mature human oocyte dysmorphisms with respect to clinical outcomes. J Assist Reprod Genet. 2016;33(8):1041-1057. https://doi.org/10.1007/s10815-016-0739-8

Sousa M, Teixeira da Silva J, Silva J, Cunha M, Viana P, Oliveira E, Sá R, Soares C, Oliveira C, Barros A. Embryological, clinical and ultrastructural study of human oocytes presenting indented zona pellucida. Zygote. 2015;23(1):145-157. https://doi.org/10.1017/S0967199413000403

Takahashi N, Kawanishi-Tabata R, Haba A, Tabata M, Haruta Y, Tsai H, Seon BK. Association of serum endoglin with metastasis in patients with colorectal, breast, and other solid tumors, and suppressive effect of chemotherapy on the serum endoglin. Clin Cancer Res. 2001;7(3):524-532. https://www.ncbi.nlm.nih.gov/pubmed/11297243

Takamizawa S, Shibahara H, Shibayama T, Suzuki M. Detection of antizona pellucida antibodies in the sera from premature ovarian failure patients by a highly specific test. Fertil Steril. 2007;88(4):925-932. https://doi.org/10.1016/j.fertnstert.2006.12.029

Ulcova-Gallova Z. Immunological and physicochemical properties of cervical ovulatory mucus. J Reprod Immunol. 2010;86(2):115-121. https://doi.org/10.1016/j.jri.2010.07.002

Yang H, Wu C, Zhao S, Guo J. Identification and characterization of D8C, a novel domain present in liver-specific LZP, uromodulin and glycoprotein 2, mutated in familial juvenile hyperuricaemic nephropathy. FEBS Lett. 2004;578(3):236-238. https://doi.org/10.1016/j.febslet.2004.10.092

Yang P, Luan X, Peng Y, Chen T, Su S, Zhang C, Wang Z, Cheng L, Zhang X, Wang Y, Chen ZJ, Zhao H. Novel zona pellucida gene variants identified in patients with oocyte anomalies. Fertil Steril. 2017;107(6):1364-1369. https://doi.org/10.1016/j.fertnstert.2017.03.029

VII. ATTACHMENTS

Attachment 1

Email of article submission

Mario Sousa

De: Tissue and Cell <EviseSupport@elsevier.com>
Enviado: 10 de agosto de 2018 19:25
Para: msousa@icbas.up.pt
Assunto: Successfully received: submission Structural and molecular analysis of the cancer prostate cell line PC3: oocyte zona pellucida glycoproteins for Tissue and Cell

This message was sent automatically. Please do not reply.

Ref: TISSUEANDCELL_2018_269
Title: Structural and molecular analysis of the cancer prostate cell line PC3: oocyte zona pellucida glycoproteins
Journal: Tissue and Cell

Dear Professor Sousa,

Thank you for submitting your manuscript for consideration for publication in Tissue and Cell . Your submission was received in good order.

To track the status of your manuscript, please log into EVISE® at:
http://www.evise.com/evise/faces/pages/navigation/NavController.jspx?JRNL_ACR=TISSUEANDCELL
and locate your submission under the header 'My Submissions with Journal' on your 'My Author Tasks' view.

Thank you for submitting your work to this journal.

Kind regards,

Tissue and Cell

Have questions or need assistance?
For further assistance, please visit our Customer Support site. Here you can search for solutions on a range of topics, find answers to frequently asked questions, and learn more about EVISE® via interactive tutorials. You can also talk 24/5 to our customer support team by phone and 24/7 by live chat and email.

Attachment 2

First page of the submission PDF

Manuscript Details

Manuscript number	TISSUEANDCELL_2018_269
Title	Structural and molecular analysis of the cancer prostate cell line PC3: oocyte zona pellucida glycoproteins
Article type	Full Length Article

Abstract

The human oocyte zona pellucida (ZP) is made of four glycoproteins, ZP1-ZP4. Recently, the prostate adenocarcinoma and prostate cancer PC3 cell-line were shown to express the human oocyte ZP3 glycoprotein, which was evaluated in a single report submitted to patenting. To further clarify if oocyte zona pellucida glycoproteins are expressed in prostate cancer tissue and PC3-cells, in the present report we evaluated protein expression of the four ZP glycoproteins in normal prostate tissue, prostate adenocarcinoma tissue and PC3-cells, and performed quantitative mRNA expression of the four ZP glycoproteins in the PC3 cell-line. Additionally, as PC3-cells have not yet been studied in detail regarding their ultrastructural characteristics, in the present report we bring forward the detailed ultrastructure of PC3-cells. PC3-cells were divided into pavement and aggregated cells. We observed new ultrastructural features in pavement and aggregated cells, with the later exhibiting two different cell types. In prostate carcinoma tissue and PC3-cells we found protein expression of the four oocyte glycoproteins, ZP1, ZP2, ZP3 and ZP4. Moreover, mRNA expression studies revealed expression of ZP1, ZP3 and ZP4 glycoproteins, but not of ZP2. Interestingly, the mRNA product of ZP1 presents intron retention.

Keywords	Electron Microscopy; Prostate Cancer; PC3 Cell Line; Zona Pellucida Glycoproteins

Corresponding Author	Mário Sousa
Corresponding Author's Institution	Institute of Biomedical Sciences Abel Salazar, University of Porto
Order of Authors	Jéssica Costa, Rute Pereira, Jorge Oliveira, Ângela Alves, Ângela Magalhães, Amaro Frutuoso, Carla Leal, Nuno Barros, Rui Fernandes, Márcia Barreiro, Alberto Barros, Mário Sousa, Rosália Sá

Suggested reviewers	Nieves Cremades, Juan Garcia-Velasco, Juan Alvarez

UNIVERSIDADE DO PORTO

FACULDADE DE **MEDICINA**